Hydrocarbon proton conducting polymers for fuel cell catalyst layers

Peron, Jennifer; Shi, Zhiqing; Holdcroft, Steven

Publisher's version / Version de l'éditeur:
https://doi.org/10.1039/c0ee00638f
Energy and Environmental Science, 4, 5, pp. 1575-1591, 2011-03-04

Energy & Environmental Science

Dynamic Article Links

Cite this: *Energy Environ. Sci.*, 2011, **4**, 1575

www.rsc.org/ees

REVIEW

Hydrocarbon proton conducting polymers for fuel cell catalyst layers

Jennifer Peron,†[a] Zhiqing Shi[a] and Steven Holdcroft*[ab]

Received 8th November 2010, Accepted 28th January 2011
DOI: 10.1039/c0ee00638f

Proton exchange membrane fuel cells (PEMFCs) employing proton conducting membranes are promising power sources for automotive applications. Perfluorosulfonic acid (PFSA) ionomer represents the state-of-the-art polymer used in both the membrane and catalyst layer to facilitate the transport of protons. However, PFSA ionomer is recognized as having significant drawbacks for large-scale commercialization, which include the high cost of synthesis and use of fluorine-based chemistry. According to published research much effort has been directed to the synthesis and study of non-PFSA electrolyte membranes, commonly referred to as *hydrocarbon* membranes, which has led to optimism that the less expensive proton conducting membranes will be available in the not-so-distant future. Equally important, however, is the replacement of PFSA ionomer in the catalyst layer, but in contrast to membranes, studies of catalyst layers that incorporate a hydrocarbon polyelectrolyte are relatively sparse and have not been reviewed in the open literature; despite the knowledge that hydrocarbon polyelectrolytes in the catalyst layer generally lead to a decrease in electrochemical fuel cell kinetics and mass transport. This review highlights the role of the solid polymer electrolyte in catalyst layers on pertinent parameters associated with fuel cell performance, and focuses on the effect of replacing perfluorosulfonic acid ionomer with hydrocarbon polyelectrolytes. Collectively, this review aims to provide a better understanding of factors that have hindered the transition from PFSA to non-PFSA based catalyst layers.

[a]*Institute for Fuel Cell Innovation, National Research Council Canada, Vancouver, British Columbia, V6T 1W5, Canada. E-mail: zhiqing.shi@nrc-cnrc.gc.ca; Fax: +1 6042213001; Tel: +1 6042213078*

[b]*Department of Chemistry, Simon Fraser University, Burnaby, British Columbia, V5A 1S6, Canada. E-mail: holdcrof@sfu.ca; Fax: +1 7787823765; Tel: +1 7787824221*

† Current address: UPMC Univ Paris 06, UMR 7574, Laboratoire Chimie de la Matière Condensée de Paris, Collège de France, 11 place Marcelin Berthelot, 75005 Paris, France. Fax: +33 14427 1504; Tel.: +33 144271545. E-mail: jennifer.peron@college-de-france.fr

1. Introduction

1.1 Overview

An increase in the worldwide use of energy sources, diminution of fossil fuels, and a realization of the environmental impact of combusting fossil fuels impose on our society a need to diversify the sources of energy utilized and a need to develop alternative energy conversion systems. Several alternative energy conversion systems exist for stationary applications but for transportation

Broader context

Proton exchange membrane fuel cell (PEMFC) technology is being aggressively developed in the context of sustainable energy conversion. PEMFCs operating with hydrogen or methanol and air or oxygen at sub-100 °C temperatures utilize a proton-conducting polymer membrane and a similar polymer in the catalyst layers (CLs). In CL, the polymer interfaces with gases, water, catalyst and its support, and with the membrane. It plays a key role in determining electrochemical kinetics, transport in the CL and the fuel cell performance. A difficult challenge on the road to PEMFCs commercialization is to increase their performance, operate at elevated temperatures and lower relative humidities, and lower costs. Less expensive, new proton-conducting polymers exhibiting increased conductivity and operational versatility are desired. Researchers are turning their attention to hydrocarbon analogues of the technologically accepted polymer, perfluorosulfonic acid ionomer. Several functionalized polyaromatic and polyheterocyclic polymers have been developed and characterized as membranes. However, there is a clear lack of information and poor understanding of how these ionomers influence PEMFC performance when employed as the proton-conducting medium in CL. This article attempts to address this deficiency by discussing studies reported in the literature, and by discussing properties required of new ionomers intended for use in CL.

only rechargeable battery technology has been utilized in volume to minimize urban pollution and lower our dependence on fossil fuels. The proton exchange membrane fuel cell (PEMFC) is another promising power converter for automotive applications but for large-scale commercialization the current technology needs improvement in terms of durability, flexibility of utilization over a wide range of operational conditions, and, most significantly, requires a significant reduction in cost. Cost targets call for $30 US per kW by 2015, with fuel cells operating with 5000 h lifetime and 60% efficiency.[1] While incremental advancements have been realized, improvements in overall fuel cell efficiency by mitigating catalyst poisoning, increasing electrochemical kinetics, utilization of less-expensive materials, and operating fuel cells with no inlet humidification and minimal gas pressure still represent significant challenges.[1] Despite the promise of improved and/or less expensive catalysts and proton conducting polymers, state-of-the-art membrane–electrode assemblies still utilize high-cost materials such as Pt and perfluorosulfonated ionomers (PFSI).

Jennifer Peron

Dr Jennifer Peron received her MSc (2004) from the National Higher School of Chemistry (Montpellier, France) and her PhD (2007) from the University of Montpellier (Institut Charles Gerhardt). From 2008 to 2010, she worked as a research associate at the Institute for Fuel Cell Innovation (Vancouver, Canada). She worked on the preparation of polymers for fuel cells, the incorporation of ionomers in catalyst-layers and on the degradation of membrane–electrodes assembly. She is currently working as a postdoc at the Laboratoire Chimie de la Matière Condensée de Paris (Paris, France) on the preparation of hybrid conducting materials for photovoltaic applications.

Zhiqing Shi

Zhiqing Shi received his MSc and BEng from the East China University of Chemical Technology, PhD degree from Simon Fraser University. From 1987 to 1998, he was a project leader for several fluoro-elastomer projects, and chief of R&D Center in Shanghai 3F New Materials Co., Ltd. (Shanghai, China). Dr Shi joined the NRC Institute for Fuel Cell Innovation in 2002 and is a Research Officer in the Membrane–Electrode-Assembly (MEA) Team. His current interests include proton exchange membranes and ionomers incorporated in catalyst layers for PEMFCs.

1.2 Catalyst layers

Electrochemical kinetics and mass transport processes associated with the catalyst layer (CL) are responsible for sharp voltage decreases when very low and very high currents are drawn, respectively. The oxygen reduction reaction (ORR) occurring at the cathode is often the rate determining electrochemical reaction in a H_2/O_2 (air) fuel cell operation and a major cause of polarization losses upon drawing current. ORR is slow compared to the considerably faster hydrogen oxidation reaction (HOR) that occurs at the anode. Exchange current densities for ORR are $\sim 10^{-10}$ A cm^{-2}, compared to 10^{-3} A cm^{-2} for HOR.[2] The inherent electrochemical activity of the catalyst, as influenced by particle size, surface morphology, electronic structure, support structure and the proton conducting phase, has a major influence on fuel cell performance.[3–5] Under high current densities, the significant volume of water produced *via* ORR must be rapidly removed from the CL in order to prevent flooding of the pore space.[6] The CL is required to facilitate the ingress of gaseous reactants and the egress of product water over its entire thickness. The relatively large thickness of the CL ($\sim$10 microns) leads to non-uniform reaction rate distributions due to impediments in gas and proton transport, which reduces the utilization of Pt catalyst.

A major advancement in CL development was demonstrated by LANL researchers in the 1980s–1990s[7] by replacement of Pt–black with Pt supported on high surface area carbon, and impregnation of the CL with a PFSA ionomer.[8,9] Pt loadings in fuel cell electrodes have subsequently been reduced from 4 mg cm^{-2} to <0.4 mg cm^{-2}. Further improvements were realized by incorporating PFSA directly into the catalyst ink, which extends the 3-D reaction zone in the electrode and increased catalyst utilization.[10,11] These concepts have been previously reviewed.[12,13] The general agreement is that $\sim$3 to 5 nm sized Pt particles deposited on a suitable carbon support are optimal.[13] However, Pt still represents more than a quarter of the overall fuel cell system cost,[14] and no replacement appears on the immediate horizon.[15]

Conventionally, a proton conducting polymer is mixed with a supported-catalyst to form a catalyst ink dispersion that is subsequently deposited onto a membrane or on a gas diffusion layer by one of several methods.[9,16] Contact between Pt and

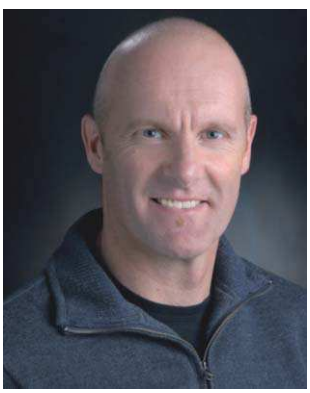

Steven Holdcroft

Prof. Steven Holdcroft received his BSc from the University of Salford, PhD from Simon Fraser University (SFU), and postdoctoral training at the University of Toronto. He is a Professor of Chemistry at SFU, and partially seconded to the National Research Council Canada —Institute for Fuel Cell Innovation where he is a research team leader and advisor. His current interests include solid polymer electrolytes, fuel cell science, π-conjugated polymers, and organic electronics.

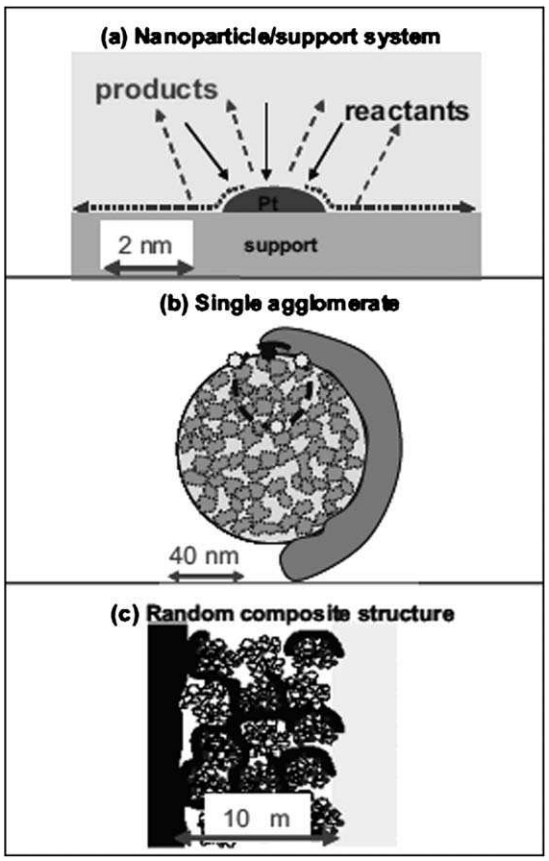

Fig. 1 Diagram illustrating the multiple length scales relevant to fuel cell catalyst layers. (a) A single supported catalyst nanoparticle; (b) an agglomerate of Pt/C particles in contact with ionomer showing primary pore space; (c) aggregates of agglomerates in the catalyst layer structure showing secondary pore space.[27] M. Eikerling, A. S. Ioselevich and A. A. Kornyshev, How good are the electrodes we use in PEFC?: (understanding structure *vs.* performance of membrane–electrode assemblies), *Fuel Cells (Weinheim, Ger.)*, 2004, **4**, 131. Copyright Wiley-VCH Verlag GmbH & Co. KGaA. Reproduced with permission.

carbon, and between carbons particles provides electronic pathways for electrical current to flow between reaction sites and the current collector. The proton conducting polymer interfaces with incoming gases, with water, with the catalyst and its support, and with the membrane. The proton conducting polymer facilitates the transport of protons necessary for ORR and HOR. The proton conducting polymer thus plays a key role in the electrochemistry of the CL—it transfers protons from inside the anode CL to the CL/proton exchange membrane (PEM) interface and from the membrane/CL interface to inside the cathode CL; it must allow reactant gases to access reaction sites and facilitate the transport of water by being both permeable and pore-forming. The polymer introduced in the CL typically possesses a high ionic conductivity, virtually no electronic conductivity, and a fine-tuned permeability and wettability. It must be chemically and interfacially compatible with the polymer constituting the PEM, and as in the case of PEMs, must be stable towards oxidation, reduction and attack by radicals, perhaps more so because of its proximity to reaction sites.

The dispersion medium used for ink preparation strongly influences the microstructure of the catalyst layer formed.[17–21] Nafion® is generally dispersed in alcoholic mixtures prior to forming the ink suspension and does not form a "true solution" but rather colloidal aggregates that may have anisotropic structure.[22,23] During fabrication, both the Pt/C and the PFSA ionomer aggregate into a complex structure. The resulting catalyst layer that is formed upon evaporation of the solvent(s) is a porous structure consisting of *primary pores* (~5 to 20 nm) that exist between agglomerates of Pt/C particles and *secondary pores* (~20 to 100 nm) that exist between aggregates of agglomerates.[24–26] It is believed that PFSA ionomer, being introduced into catalyst solution as a dispersion in alcohol, is mainly deposited in secondary pores, on the surface of Pt/C aggregates without being able to penetrate the primary pores. These main structural features are illustrated in Fig. 1.[27]

Despite the infancy in the general understanding of how catalyst inks are formed at the molecular level from agglomerates and aggregates of agglomerates, it can be expected that a transition to hydrocarbon polyelectrolytes from PFSA ionomer will lead to radical deviations in aggregation processes, which ultimately will determine the particulate structure of the ink and catalyst layer, and ultimately influence the fuel cell performance of the catalyst layers.

1.3 Proton exchange membranes

Long side chain perfluorosulfonic acid (PFSA) ionomers, such as Nafion®, have been studied for more than 50 years.[22] PFSAs possess a high ionic conductivity while maintaining moderate water uptake up to 100 °C under high relative humidity (RH).[28] Their desirable properties exhibited for PEM applications are attributed to the internal nanostructure in which the sulfonic groups arranged as hydrophilic channels in an amorphous phase are separated by partially crystalline domains of hydrophobic Teflon®-like segments.[29–31] While PFSA ionomers exhibit excellent chemical and mechanical stability, they are expensive, highly permeable to methanol (and largely unsuitable for DMFCs),[32] and their glass transition temperature occurs at 90–110 °C,[22] which is below the operational temperature preferred by the automotive industry. Durability studies have shown that PFSI degrades in the presence of radicals, and moreover, reaction products exacerbate the dissolution and transport of Pt from the CL into the membrane.[33–36] Short side chain PFSA is considered a promising material to replace long-side chain PFSA both as a membrane[37–40] and in the CL,[41] though the cost of these materials is still a substantial issue for their integration into the commercialization of PEMFCs.

Hydrocarbon-based polyaromatic and polyheterocyclic polymers, including polyethersulfones, polyetherketones, polystyrene, polybenzimidazoles, and polyimides, are being investigated as candidates for replacing PFSA ionomer as a fuel cell *membrane* because they are potentially less expensive. Hydrocarbon polymers can be easily functionalized during synthesis, or post-sulfonated to provide a wide range of ion exchange capacity (IEC) membranes. Water uptake of the membranes is commensurate with the degree of sulfonation. As proton conduction is water-assisted, the conductivity of sulfonated polyaromatic membranes is highly dependent on the IEC, as is methanol permeability, which is often lower than Nafion®.[42] The permeability of the membranes to hydrogen and

oxygen is also lower. From a structural point-of-view, polyaromatics differ from PFSA ionomers not only because of the main chain but also because in the majority of instances the sulfonic groups are directly attached to the polymer backbone. This restricts the separation of the hydrophilic acid from the hydrophobic backbone, and hence phase segregation is less pronounced.[43] Furthermore, the pK_a of the sulfonic acid group attached to a polyaromatic polymer lies between −2 and −1,[44] *i.e.*, it is a much weaker acid than that attached to PFSA (pK_a −6). Thus in order to reach a conductivity similar to PFSA, polyaromatic polymers require much higher degrees of functionalisation. This imparts negative attributes. For example, the non-hydrated polymers are often much more brittle, highly sensitive to relative humidity, and prone to dehydration. Hence, their conductivity may drop dramatically under reduced RH. "Water-free", acid-doped polymers are materials being considered for operation at temperatures above 150 °C, the most advanced PEM being based on phosphoric acid-doped polybenzimidazoles which reportedly performs respectably at temperatures as high as 180 °C under no external humidification.[45] However, the production of water during the electrochemical reaction can lead to the elution of unbound acid and irreversible loss of proton conduction. The properties of polyaromatics as a *fuel cell membrane* have been extensively reviewed in the literature[43,46–51] and are not reviewed further here. In this review, we address the issue of utilizing hydrocarbon polyelectrolytes in fuel cell *catalyst layers*, and in particular the properties of the polymer electrolyte that are relevant to their utilization in a CL.

1.4 Alternative proton conducting polymers for use in catalyst layers

If the proton conducting polymer employed in the catalyst layer is substantially different to that employed in the membrane then, in addition to the formation of an interfacial mass transport resistance, the difference in physical properties of the two materials, *e.g.*, hydrophilicity/hydrophobicity, IEC, water content, *etc.*, may lead to premature delamination of the membrane–electrode-assembly (MEA) during fuel cell operation.[52–54] Thus the development of new proton conducting polymers for membranes ought to be complemented by the development of similar polymers for use in catalyst layers—but the latter has considerably lagged the former. Perhaps this is because of a perception that having developed an alternative hydrocarbon proton conducting polymer it would be a simple matter to incorporate it in the catalyst layers to prepare MEAs—as is conventionally carried out with PFSAs. Unfortunately, due to the complexity of the catalyst layer and the influence of the components on the physical properties of the catalyst layer, *e.g.*, porosity, pore size distribution, wettablity, active surface area, *etc.*, this simple analogy is not borne out experimentally. It has been demonstrated that simple changes in composition of the catalyst ink, *e.g.*, dispersion medium, carbon support, ionomer content, have a significant influence on the electrochemical properties of the catalyst layer.[26,55] In this context, replacing the proton conducting polymer in the catalyst ink should be construed as a significant perturbation to the current protocol ascribed to the preparation of catalyst inks and catalyst layers.

The peer-reviewed literature concerning hydrocarbon polymer electrolytes being used in fuel cell catalyst layers is relatively sparse and focuses largely on the investigation of sulfonated polyarylene ionomers that have been prepared for PEM materials. These include sulfonated poly(etherketones),[56–66] polysulfones (PSU),[67,68] poly(ethersulfones),[52,67–71] and polyheterocyclics such as polyimides (PI),[72,73] polybenzimidazoles (PBI),[74–77] and polyphosphazene.[78] Representative structures of these families of polymer are presented in Fig. 2. These reports confirm the importance of the relationship between the sulfonated hydrocarbon polymer content, the number of proton exchange sites, the electrochemistry of the catalyst layer, and fuel cell performance. Due to the differences in the deposition methods used (brushing, spraying, decal transfer), in the preparation methods of the MEA (catalyst coated gas diffusion layer *vs.* catalyst coated membrane), the choice of solvents, membranes, and polymer IEC, and also because of the differences in fuel cell testing conditions employed (gas, pressure, temperature, humidity) it is folly to compare the results obtained by different research groups. However, general trends are emerging. Table 1 summarizes peer-reviewed research dedicated to this topic, and lists the membrane, the proton conducting polymer at the cathode, and for comparison, the potential/current density reported in the intermediate current density region where the cell potential decreases linearly with current density.

Several groups have examined the influence of the proton conducting polymer contents in the CL. A few research groups have also studied the influence of IEC of the polymers on fuel cell performance. The proton conducting polymers (measured as a membrane) generally exhibit proton conductivities similar to Nafion® (>10^{-2} S cm^{-1} at rt and 100% RH); however, they usually possess larger degrees of hydration under comparable RH due to their larger IEC (*e.g.*, >1.3 meq g^{-1} for sulfonated polyetheretherketone (sPEEK)). It can be seen from Table 1 that the performances of MEAs prepared with polyaromatic or polyheterocyclic polyelectrolytes are generally lower than state-of-the-art materials prepared with PFSA ionomers. This is generally the result of a large overpotential observed at low

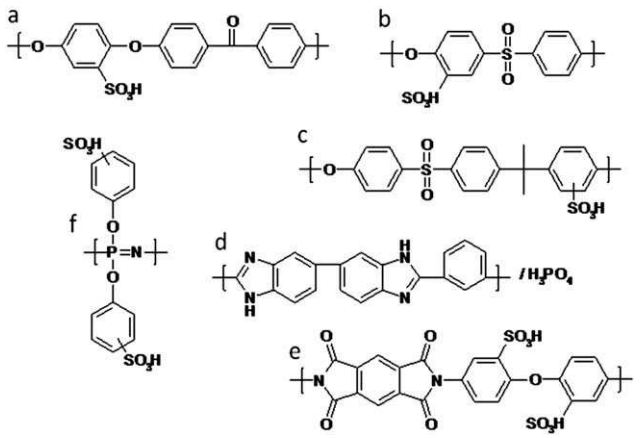

Fig. 2 Example of ionomers introduced in CL: (a) sulfonated polyetheretherketone, (b) sulfonated polyethersulfone, (c) sulfonated polyarylethersulfone, (d) polybenzimidazole/phosphoric acid, (e) sulfonated polyetherimide, (f) sulfonated poly(phenoxyphosphazene).

Table 1 Summary of performance of MEAs containing hydrocarbon ionomer in the cathode catalyst layer

Ref	Cathode ionomer	IEC (meq g^{-1})/D.S. (%) (optimum*)	Loading (optimum*)	Membrane	Conditions	Performance in the ohmic region	Ratio catalyst/support catalyst loading at the cathode
Sulfonated polyetheretherketone (sPEEK)							
56	sPEEK	1.74 meq g^{-1}	30%*	sPEEK	75 °C, H_2/air 100% RH, P atm	0.58 V @ 0.5 A cm^{-2}	Pt/C 40%, Pt 0.4 mg cm^{-2}
57	sPEEK	1.88* meq g^{-1}	15%*	Nafion® 117	35 °C, H_2/O_2 100% RH, P atm	0.25 V @ 0.1 A cm^{-2}	Pt/C 20 wt%, Pt 0.25 mg cm^{-2}
58	sPEEK	2.1* meq g^{-1}	30%	sPEEK, 1.75 meq g^{-1}	80 °C, H_2/air 75% RH, P_{H_2} 0.65 atm, P_{O_2} 0.136 atm	0.49 V @ 0.1 A cm^{-2}	Pt/C 40 wt%, Pt 0.4 mg cm^{-2}
59	sPEEK	2.1* meq g^{-1} 1.75 meq g^{-1}	30% 15%*	sPEEK, 1.75 meq g^{-1}	80 °C, H_2/air 75% RH, P atm	0.57 V @ 0.1 A cm^{-2} 0.6 V @ 0.1 A cm^{-2}	Pt/C 40 wt%, Pt 0.4 mg cm^{-2}
60	sPEEK	65%	30%	Nafion® 112	65 °C, H_2/air RH n.a., P atm	0.61 V @ 0.3 A cm^{-2}	Pt/C 60 wt% Pt, Pt 0.48 mg cm^{-2}
61	sPEEK	1.4 meq g^{-1}	20%	Nafion® 211	80 °C, H_2/O_2 100% RH, P atm	0.52 V @ 1 A cm^{-2}	Pt/C 46.3 wt%, Pt 0.4 mg cm^{-2}
62	sPEEK–PEG porous	60%	30%	Nafion® 112	65 °C, H_2/air 100% RH, P atm	0.6 V @ 0.3 A cm^{-2}, improved mass transport	Pt/C 60 wt%, Pt 0.3 mg cm^{-2}
63	sPEEK–PTFE 10%	1.9 meq g^{-1}	10%	sPEEK	50 °C, H_2/O_2 100% RH, P atm	0.52 V @ 0.3 A cm^{-2}	Pt/C 20 wt%, Pt 0.25 mg cm^{-2}
53	sPEEK	60%	n.a.	sPEEK	30 °C, MeOH 2 M/O_2 RH n.a., P. n.a.	0.3 V @ 0.1 A cm^{-2}	Pt–black 5 mg cm^{-2}
122	sPEEK	61%	5%	sPEEK	60 °C, MeOH 2 M/O_2 RH n.a., P. n.a.	0.5 V @ 0.2 A cm^{-2}	Pt–black 5 mg cm^{-2}
65	sPEEK	1.33 meq g^{-1}	20%	sPEEK1.33/PSF-ABIm 3% blend	65 °C, MeOH 1 M/O_2 RH n.a., P atm	0.34 V @ 0.1 A cm^{-2}	Pt/C 20 wt%, Pt 1 mg cm^{-2}
64	sPEEK	1.33* meq g^{-1}	20*	Nafion® 115	65 °C, MeOH 1 M/O_2 RH n.a., P atm	0.15 V @ 0.22 A cm^{-2}	Pt/C 20 wt%, Pt 1 mg cm^{-2}
Other polyaromatics and polyheterocyclic for low temperature PEMFCs							
66	sPEKK	1.4 meq g^{-1}	25%	sPEKK 1.4	80 °C, H_2/O_2 75% RH, P atm	0.68 V @ 1 A cm^{-2} (IR free)	Pt/C 46.5 wt%, Pt 0.4 mg cm^{-2}
113	SPE	2.17* meq g^{-1} 1.61 meq g^{-1}	0.7 *I*/*C* 1 *I*/*C**	Nafion® 112 Nafion® 112	80 °C, H_2/O_2, 100/25% RH, P atm	0.71 V @ 0.5 A cm^{-2} 0.7 @ 0.5 A cm^{-2}	Pt/C 45.8 wt%, Pt 0.5 mg cm^{-2}
73	sPI	1 meq g^{-1}	33% *	Nafion® 112	80 °C, H_2/O_2, 100/25% RH, P atm	0.62 V @ 0.5 A cm^{-2} (IR free)	Pt/CB 46.3%, Pt 0.5 mg cm^{-2}
52	sPAES	40%	7%	sPAES	30 °C, MeOH n.a./O_2	0.3 V @ 0.1 A cm^{-2}	Pt 5 mg cm^{-2}
70	SPAE	1.8 meq g^{-1}	I/C 0.7	Nafion® 212	80 °C, H_2/air 78% RH, P atm	0.75 V @ 0.28 A cm^{-2} (IR free)	Pt/C 68%, Pt 0.5 mg cm^{-2}
69	SPAE	2.5 meq g^{-1}	I/C 0.7	Nafion® 212	80 °C, H_2/O_2 78% RH, P atm	0.7 V @ 0.65 A cm^{-2} (IR free)	Pt/C 47.9%, Pt 0.5 mg cm^{-2}
67	sPSU-50	0.95 meq g^{-1}	20%	Nafion® 112	120 °C, H_2/O_2 100% RH, P 0.8 bar	0.7 V @ 0.5 A cm^{-2} (IR free)	Pt/C 20%, Pt 0.08 mg cm^{-2}
68	SPSU	1.55 meq g^{-1}	20%	SPSU	120 °C, H_2/O_2 100% RH, P 2 bar	0.62 V @ 0.5 A cm^{-2} (IR free)	Pt–CB 20 wt%, Pt 0.1 mg cm^{-2}
71	sPES-40	1.47 meq g^{-1}	0.9 mg cm^{-2}	sPES-40	70 °C, H_2/O_2 100% RH, P 60/50 psi	0.5 V @ 0.9 A cm^{-2}	n.a.
117	PES F-PES	60% 60%	2%* 2%*	PES F-PES	70 °C, H_2/O_2 100% RH P atm	0.59 V @ 0.2 A cm^{-2} 0.56 V @ 0.2 A cm^{-2}	Pt/C 40% Pt 0.4 mg cm^{-2}
78	sPOP	1.58 meq g^{-1}	15%	Nafion® 212	80 °C, H_2/air humid., P atm	0.58 V @ 0.6 A cm^{-2}	Pt/C 40 wt%, Pt 0.4 mg cm^{-2}
Polybenzimidazole for high temperature PEMFCs							
74	PBI/H_3PO_4	$6H_3PO_4$/PBI unit	20%	AB-PBI–H_3PO_4	150 °C, H_2/O_2, P n.a.	0.45 V @ 0.5 A cm^{-2}	Pt/C 20%, Pt 0.4 mg cm^{-2}
76	PBI	n.a.	n.a.	PBI–H_3PO_4	180 °C, H_2/O_2, P atm	0.5 V @ 0.3 A cm^{-2}	Pt/C 40%, Pt 0.4 mg cm^{-2}
75	PBI	—	0.75 mg cm^{-2}	AB-PBI $3.7H_3PO_4$	160 °C, H_2/O_2 0%, P n.a.	0.5 V @ 0.28 A cm^{-2}	Pt/C 20 wt%, Pt 0.45 mg cm^{-2}
77	PBI/H_3PO_4	12–15H_3PO_4/PBI unit	0.7 mg cm^{-2} PBI	PBI–$6H_3PO_4$	200 °C, H_2/O_2, dry gases, P n.a.	0.6 V @ 0.5 A cm^{-2}	Pt/C 20 wt%, Pt 0.5 mg cm^{-2}

current densities, *i.e.*, the kinetic region. Polyaromatic and polyheterocyclic-based electrodes confer lower electrochemical surface area (ESA) to the catalyst layer. Further details are presented later in this review, along with a discussion of the influence of IEC and polymer content. The following sections discuss properties relevant for the utilization of hydrocarbon polyelectrolytes in CLs and include gas permeability and ORR kinetic parameters, the morphological structure of the CL, the influence of polymer content and ion exchange capacity, the influence of dispersion media, and lastly, the durability of hydrocarbon polyelectrolytes.

2. ORR kinetics and mass transport (*ex situ* analyses)

2.1 Kinetics

The kinetics of ORR on Pt in the presence of a proton conducting polymer electrolyte is expected to be strongly influenced by the nature of the polymer. This section describes the use of *ex situ* electrochemical techniques to extract kinetic information. However, it should be borne in mind that data are extracted from techniques performed on the membrane form of the polymer, and therefore might not be directly applicable to polymers dispersed in a CL; but the trends observed are informative.

Using a solid state microelectrode system, ORR kinetic parameters including exchange current densities, j_d, Tafel slopes, and α transfer coefficients can be extracted from slow sweep voltammetry data. Zhang *et al.*[79] report dual Tafel slopes for ORR in Nafion® 117 and sulfonated poly(arylene ether sulfone) with 40% sulfonated groups/repeat units (SPES-40). The values are ~ -70 mV dec^{-1} under low current density (lcd) and range between -117 and -125.6 mV dec^{-1} under high current density (hcd) for Nafion® 117; and between -83.7 and -88.7 mV dec^{-1} for lcd and between -144.4 and -147.7 mV dec^{-1} for hcd for SPES-40. The α values were found to be independent of temperature and also exhibit deviations from the characteristic values for both membranes being $\sim$0.9 and $\sim$0.55 for Nafion® and $\sim$0.75 and $\sim$0.45 for SPES-40 under lcd and hcd conditions, respectively. In both regions, the membranes exhibit similar exchange current densities although SPES-40 membranes showed slightly higher values than Nafion®, and the current density increased with temperature. Similar trends were observed with polysulfone post-sulfonated. Astill *et al.*[63] also report the observation of dual Tafel slopes corresponding to oxide-covered and oxide-free Pt surface in the case of sPEEK 1.9 meq g^{-1} and larger kinetic limitations than in the case of Nafion®. Tafel slopes at low and high current densities were also observed to be higher in the case of the polyaromatic polyelectrolytes, in comparison to Nafion®. At 303 K, 100% RH and 30 psi, the slopes for sPEEK were -73 and -125 mV dec^{-1}, and –55 and -83 mV dec^{-1} for Nafion® under low and high current densities, respectively. In the case of sPEEK, Easton *et al.*[57] reported a much lower exchange current density compared to Nafion® ($\sim$50 nA *vs.* 410 nA). At 303 K, the lcd exchange current density for Nafion® was reported to be 1.8×10^{-10} A cm^{-2}, while for sPEEK's it was 5.7×10^{-11} A cm^{-2}, thus the rate of oxygen reduction at the Pt|Nafion® interface is much greater. The lower exchange current density for sPEEK and larger Tafel slope will result in larger kinetic limitations in fuel cell cathodes, which is observed experimentally in fuel cells.[57] As with the oxygen permeability, the ORR limiting current in sPEEK membranes increases with IEC. However, in comparison to Nafion® 117, the limiting currents are significantly lower for all IEC sPEEK membranes due to the significantly reduced solubility of oxygen.[80]

Miyatake *et al.*[81] used rotating disk electrode experiments to study ORR parameters at the interface of Pt/carbon black and sulfonated polyimide (SPI). They find that the polymer thickness must be <0.05 microns to reduce errors to <25% deviation from purely kinetically controlled ORR under flooded conditions at 0.8 V. They also studied hydrogen peroxide formation during ORR and found that the formation of H_2O_2 in SPI is much slower than in Nafion® (*e.g.*, the hydrogen peroxide yield was 0.44%, 0.12%, and 0.03% for SPI *vs.* 0.56%, 0.20%, and 0.10% for Nafion® at 0.7, 0.76 and 0.8 V, respectively), which is a favourable result in the context of the stability of MEAs to fuel cell operation.

Although PBI is not directly involved in the oxygen reduction reaction, the presence of PBI in the electrolyte can affect both the availability of oxygen on catalyst adsorption sites and the oxygen solubility in the electrolyte. Liu *et al.*[82,83] studied ORR kinetics parameters using a micro-band electrode. Tafel slopes obtained at 150 °C/10% RH for H_3PO_4 doping levels ranging from 4.5 to 10 ranged from -92 to -104 mV dec^{-1}, while the exchange current density ranged from 1.8×10^{-9} to 2.4×10^{-8} A cm^{-2}. Tafel slopes of $\sim$100 mV dec^{-1} are similar to Tafel slopes reported for ORR on Pt in conc. phosphoric acid. For ORR at Pt the effect of the PBI in PBI–H_3PO_4 electrolytes on the adsorption on Pt is deemed minimal because of the dominant adsorption of phosphoric acid and its derivate anions. For oxygen reduction at Pt interfaced with H_3PO_4 or PBI–H_3PO_4, a change in adsorption coverage on the Pt surface is unlikely because of strong adsorption of phosphoric acid and its anions, therefore the adsorption of reactant intermediates follows a Temkin isotherm over the whole potential region examined. By studying the exchange current density as a function of oxygen saturation concentration and water content, it was found in both cases that ORR is first order. According to these results Liu *et al.* state that in PBI–H_3PO_4 systems, ORR is first order with respect to the oxygen saturation and proton concentration in the electrolyte.[82,83]

2.2 ORR mass transport parameters—O_2 permeability (*ex situ* analyses)

An important property of the polymers regarding their application in catalyst layers is the dissolution of oxygen and the diffusivity and permeability of oxygen. As a membrane, the permeability to oxygen (and hydrogen) should be as low as possible to limit the crossover of reactant gas(es). Gas permeation across the membrane is responsible for a decrease in gas partial pressure at both the anode and the cathode and contributes to degradation of the MEA.[36,84] In contrast, as a proton conducting medium in the CL, the permeability to oxygen (and hydrogen) should be maximized in order to promote transport of reactant gas to the reaction sites. This creates a paradox if the same proton conducting polymer is used as both

the membrane *and* in the CL. The permeability of a membrane to a gas can be expressed as the product of the diffusion coefficient D ($cm^2\ s^{-1}$) and the solubility in the polymer C ($mol\ cm^{-3}$). These parameters play a significant role, for example, in the limiting current density for oxygen reduction, as evident from Fick's first law shown in eqn (1), where it can be seen that the limiting current density increases with the solubility and diffusion coefficient of oxygen. The general consensus is that diffusion occurs most rapidly in the hydrophilic domains of the polyelectrolyte while the O_2 solubility is highest in the hydrophobic regions.[85–89] Nafion® 117 permeability values obtained using different experimental setups have been previously reviewed.[90,91]

$$i_l/nF = (Dc_b)/t \quad (1)$$

where i_l is the limiting current density, n is the number of electrons transferred per mole, F is the Faraday constant, D is the oxygen diffusion coefficient, c_b is the oxygen solubility in the electrolyte, and t is the thickness of the mass transfer boundary layer.

Methods used to determine gas permeability include: analysis of permeation rates through the membrane under a given gas pressure difference (volumetric methods, time lag-techniques), electrochemical monitoring techniques (EMT), and micro-electrode methods. Permeability values obtained from volumetric and electrochemical monitoring techniques cannot directly be compared. Due to the difficulty of the experiment and the sensitivity of the results to the experimental conditions, the values obtained by different groups are also difficult to compare.

2.2.1 Volumetric measurements. Watanabe reports H_2 and O_2 permeability values obtained using volumetric measurements coupled with gas chromatography for a series of sulfonated polyimides[92,93] and polyaromatics polymers.[94] The gas permeability of these different polymers, measured over a wide range of temperatures and RH, is found to be lower than that of Nafion® membranes. For example, the O_2 permeability coefficient through a polyimide copolymer containing 1*H*-1,2,4-triazole groups in the main chain is found to be in the range of 10^{-11} to 10^{-10} $cm^3\ cm\ cm^{-2}\ s^{-1}\ cmHg^{-1}$ at 80 °C over the range of RH 0–95%, while the oxygen permeability coefficient measured for Nafion® 212 was found to be between 10^{-9} and 10^{-8} $cm^3\ cm\ cm^{-2}\ s^{-1}\ cmHg^{-1}$.[93] The permeabilities of sPEEK with sulfonated poly(oxa-*p*-phenylene-3,3-phthalido-*p*-phenylene-oxyphenylene groups) (dry gas permeability measured at 25 °C)[95] and PBI membranes (measured at 80 °C)[96] are also reported to be lower than that of Nafion®. A hydrogen permeability of 1.6–4.3 × 10^{-17} $mol\ cm\ cm^{-2}\ s^{-1}\ Pa^{-1}$, and an oxygen permeability value of 5–10 × 10^{-19} $mol\ cm\ cm^{-2}\ s^{-1}\ Pa^{-1}$ are reported for PBI–Celanese membranes between 80 °C and 180 °C;[96] however, for membranes doped with phosphoric acid the oxygen and hydrogen permeability measured at 80 °C was higher than that of Nafion® ($P_{O2,\ PBI}$: 30 × 10^{-17} $mol\ cm\ cm^{-2}\ s^{-1}\ Pa^{-1}$, $P_{O2Nafion®}$: 3.1 × 10^{-17} $mol\ cm\ cm^{-2}\ s^{-1}\ Pa^{-1}$)—this increase being due to swelling of the membrane and separation of the polymer chains. Kumbharkar *et al.*[97] reported that the introduction of bulkier groups in PBI, such as hexafluoroisopropylidene, leads to a decrease in chain packing density and an enhancement of gas diffusion. Muldoon *et al.*[78] measured the oxygen permeability through Nafion® and sulfonated polyphosphazene membranes. They evidenced an increase of the activation energy for oxygen permeation with increasing 4-phenylphenoxy content. Between 23 and 40 °C, they reported lower permeability values for polymers with higher IEC but for a given IEC the permeability values are lower than those of Nafion®, although, by extrapolation it is claimed that the oxygen permeability would be higher than in Nafion® above 55 °C.

2.2.2 Electrochemical monitoring techniques. The electrochemical monitoring technique allows determination of solubility and diffusion coefficients separately. Mass transport properties and kinetic parameters associated with ORR in perfluorosulfonic membranes such as Nafion® using a solid state cell have been extensively studied.[89,98–100] Holdcroft and co-workers[101–103] expanded upon the relationship between chemical composition and the mass transport properties by studying a series of sulfonated trifluorostyrene polymers (BAM®) (equivalent weight-EW 407–735 g mol SO_3H^{-1}), sulfonated styrene–(ethylene–butylene)–styrene copolymers (DAIS-Analytical) (EW 585–1062 g $mol_{SO_3H}{}^{-1}$) membranes and sulfonated polyetherketones;[57,63] and Mukerjee's group[79,104,105] report the properties of sulfonated polysulfone derivatives. These groups studied gas transport properties in various membranes as a function of IEC, temperature, pressure and RH. Membranes exhibit the same dependence to pressure and temperature as Nafion®. Henry's Law is obeyed, *i.e.*, the oxygen solubility increases with pressure, the diffusion coefficient increases and O_2 solubility decreases with temperature. Because the increase in diffusion coefficients is more pronounced than the decrease in solubility, the overall membrane permeability increases with temperature. Nafion® membranes exhibit a much greater increase in permeability with temperature compared to other membranes. In addition to the expected increase in diffusion of gases with temperature, an increase in temperature is believed to enhance the motion of polymer segments, in turn increasing the free volume within the polymer. O_2 is believed to diffuse mainly through the hydrophilic domains, while the solubility of this gas is enhanced in highly fluorinated hydrophobic regions. Supporting this assertion, for example, the activation energy of O_2 dissolution in sPEEK (11.7 kJ mol^{-1}) is lower than in Nafion® (14.9 kJ mol^{-1}).

Oxygen diffusion coefficients and solubilities measured under the same temperature and RH are presented in Table 2. It can be seen in Table 2, that for PAN-*g*-macPSSA, PS-*g*-macPSSA, ETFE-*g*-PSSA, PVDF-*g*-PSSA,[106] sPEEK[57] and sPES[104] membranes the diffusion coefficient, D_{O_2}, increases and solubility, C_{O_2}, decreases when IEC is increased. This phenomenon is also observed for PFSA ionomers where it is attributed to faster oxygen diffusion dynamics in aqueous domains compared to hydrophobic perfluorinated backbone domains.[89,107] Although the permeability of the sulfonated hydrocarbon membranes increases with increasing IEC, the resulting oxygen permeability for all IEC membranes is found to be lower compared to Nafion® (Nafion® 117). For sPEEK membranes, the substantially lower permeability is largely due to the considerably lower oxygen solubility, which is related to the absence of highly hydrophobic regions. For sulfonated polysulfide sulfone (sPSS) membranes, despite their high water content, Zhang *et al.*[104]

Table 2 Polymer oxygen diffusion coefficient and solubility measured using electrochemical solid state cell. Measurement performed at 323 K under 100% RH[a]

Ref.	Polymer	*P*/atm	IEC/meq g^{-1}	$D_b \times 10^6$/cm^2 s^{-1}	$c_b \times 10^6$/mol cm^{-3}	$D_b c_b \times 10^{12}$/mol cm^{-1} s^{-1}
63	N117	2	0.9	12.4	5.7	70.7
63	sPEEK	2	1.9	10.7	1.1	11.9
79	N117	1	0.9	2.17	6.68	14.52
79	SPES-40	1	1.72	2.08	2.39	4.97
105	N117	3	0.9	5.51	9.42	51.88
105	SPES-40	3	1.47	3.34	5.69	19.04
105	SPES-PS	3	1.5	4.88	7.06	34.51
104	N117	3	0.9	5.51	9.42	51.88
104	SPES-30	3	1.2	2.2	10.54	23.23
104	SPES-60	3	2.2	10.34	3.47	35.91
104	SPSS-20	3	0.7	0.22	15.21	3.4
104	SPSS-50	3	1.8	3.69	3.41	12.61
106	PAN-*g*-macPSSA	3	1.15	3.7	1.9	7
106	PAN-*g*-macPSSA	3	1.76	17.8	2.3	41
106	PAN-*g*-macPSSA	3	1.85	15.6	1.8	28
106	PS-*g*-macPSSA	3	1.04	0.8	14.1	11
106	PS-*g*-macPSSA	3	1.38	4	8.3	33
106	PS-*g*-macPSSA	3	1.68	1.7	9.6	16
106	PVDF-*g*-PSSA	3	1.37	4.7	3.2	15
106	PVDF-*g*-PSSA	3	3.06	17.9	3.4	61
101	N117	3	0.91	9.3	5.5	51
101	ETFE-*g*-PSSA	3	2.13	8.3	3.8	32
101	ETFE-*g*-PSSA	3	3.27	16.6	3.3	54
103	N117	3	0.9	9.76	7.53	73.5
103	BAM3G 407	3	2.46	40.6	1.75	71

[a] Polymer IECs were selected from a series of IEC measurements.

found a smaller diffusion coefficient than for Nafion® 117. The water-filled channels connecting the hydrophilic ionic clusters within the polyaromatic membranes appear to make important contributions to the process of O_2 diffusion.

A modified version of the solid-state cell, using a micro-band electrode, was proposed by Wainright and Savinell *et al.*[82,83] and used to measure both mass transport and kinetic parameters for phosphoric acid doped-PBI systems. Using the micro-band electrode technique, Liu *et al.*[82] studied the influence of the doping level on the permeability of PBI–H_3PO_4 membranes. Their study suggests that the oxygen diffuses mainly through the amorphous H_3PO_4 phase, and hence is enhanced by increasing the doping level. At 150 °C, 10% RH, when the doping level is increased from 4.5 to 10 H_3PO_4 molecules per PBI repeat unit, the solubility and diffusion coefficients increase from 0.57×10^6 to 1.13×10^6 mol cm^{-3} atm^{-1} and from 2.8×10^{-6} to 8×10^{-6} cm^{-2} s^{-1}, respectively. The oxygen solubility coefficient is higher than expected for pure phosphoric acid under these conditions; the authors[82] attribute this to the presence of crystalline PBI regions.[102,107,108]

2.2.3 ***In situ*** **measurements.** Since neither the volumetric nor electrochemical methods reflect gas permeation through materials under realistic fuel cell conditions, a number of groups have developed specific techniques to measure oxygen permeability in fuel cells or simulated setups. Hydrogen permeability measurement across MEAs in fuel cell setups is a well established technique.[90] Using *in situ* fuel cell techniques, Sambandam and Ramani[109] confirm the much lower oxygen permeability of sPEEK membranes in comparison to Nafion®, and Ayad *et al.* studied the effect of different proton conducting polymers on the kinetics of ORR by determining the permeability of oxygen in films at the surface of a platinum disc using rotating disk electrode in sulfuric acid.[110] For experiments carried out at 25 °C, the oxygen permeability is reported to be 9×10^{-12} mol cm^{-1} s for Nafion®, 2.5×10^{-12} mol cm^{-1} s for sPEEK, 10^{-12} mol cm^{-1} s for SPI, and 0.5×10^{-12} mol cm^{-1} s for non-functionalized PBI. These data also confirm that oxygen permeability through Nafion® is much faster than through sulfonated hydrocarbons despite the latter's higher IEC and higher water content.

3. Catalyst layer structure, fuel cell performance and electrochemical properties

3.1 Influence of polymer content

The fullest utilization of Pt is obtained when the surface area in contact with the electrolyte is maximized and the catalyst structure is sufficiently porous to allow facile transport of reactant gas to the interior of the catalyst layer. Poor wetting of the catalyst, or electrical isolation of the Pt will diminish its effectiveness. Hence the percentage of the polymer electrolyte in the catalyst layer is an important variable: too little, the Pt is insufficiently wetted; too much, Pt particles may be isolated, and in addition, excessive wetting may flood the porous structure thus inhibiting reactant transport. The optimum ionomer content for Nafion® based CLs is typically 30 to 35 wt%.[17,20,111,112] Furthermore, the form of the proton conducting polymer in the dispersion and subsequently in the catalyst ink should be considered, *i.e.*, does the polymer exist as isolated chains, or small or large aggregates? For example, poorly soluble PFSA ionomers, with their linear fluorous segments, tend to aggregate in dispersions, which may

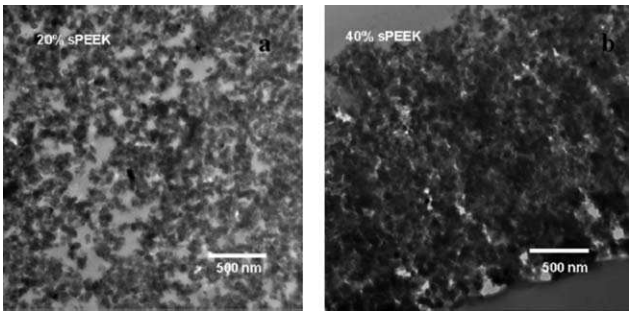

Fig. 3 TEM of sulfonated poly(ether ether ketone-based catalyst layers: 20 wt% sPEEK content (left); and 40 wt% sPEEK content (right)).[61] Reproduced with permission from *J. Electrochem. Soc.*, **157** (8), B1230 (2010). Copyright 2003, The Electrochemical Society.

limit the penetration of single polymer chains into the primary pores of Pt/C aggregates, and promote their inclusion (as aggregates) into the secondary pores. Highly soluble polymer chains on the other hand may exist in solution as weakly bound aggregates or as single chains that may penetrate the primary pores of Pt/C aggregates; the extent of this process will be strongly influenced by specific properties of the polymer such as the molecular flexibility of individual chains, the interaction of the polymer with Pt and the carbon support, *etc.*, and is expected to have a profound impact on fuel cell performance. To date such interactions, polymer–polymer and polymer–Pt/C, especially those involving hydrocarbon proton conducting polymers are under-studied.

When considering sulfonated polyaromatic-based catalyst layers the optimal polymer electrolyte content should be carefully considered because of the potentially different CL morphology and pore size distribution that may result. von Kraemer *et al.*,[68] for example, observed highly porous catalyst layers when the sulfonated polysulfone (SPSU) content is <20 wt% whereas the porosity was drastically reduced for polymer contents >30 wt%. sPEEK-based CLs are also reported to be denser and less porous than Nafion® analogues of equivalent mass content.[56,61] As a consequence of increased densification with increased sulfonated hydrocarbon content, the CL thickness is reduced. For instance, Peron *et al.*[61] report a thickness decrease of the CL from 10 to 4 microns when the sPEEK loading is increased from 20 to 40 wt%, as illustrated in Fig. 3.

Kim *et al.*[74] studied the impact of increasing the H_3PO_4/PBI content in catalyst layers on poly(2,5-benzimidazole) (AB-PBI) membrane-based MEAs using SEM and BET analysis. Increasing the H_3PO_4–PBI content leads to a systematic reduction of both the primary and secondary pore space, consistent with densification of the CL. In the case of sulfonated polyimides (SPIs), Higuchi *et al.*[73] found that the primary pore (<100 nm) volume decreases as the polymer to carbon black ratio is increased, while the secondary pore (>100 nm) volume increases. In contrast to the above, they found that the thickness of these CLs increases from 20 microns to 35 microns when the polymer to carbon black mass ratio is increased from 0.5 to 1.5. It is worth noting that the sulfonated polyimide studied by Higuchi *et al.* is a much more bulky, rigid copolymer, compared to sulfonated polyetheretherketone, sulfonated polysulfone and polybenzimidazole, and hence may block primary pore space.

Beleke *et al.*[113] observed, by STEM, that in sulfonated polyether (SPE)-based catalyst layers, Fig. 4, a thin layer (a few nanometres thick) of polymer locates on the outer edges of Pt/C aggregates, in regions where no Pt catalyst particles exist. They observed complete coverage of Pt/C by SPE when the polymer content is 30 wt% or greater (SPE/C ratio > 1). The pore size distribution analysis, performed using mercury porosimetry,

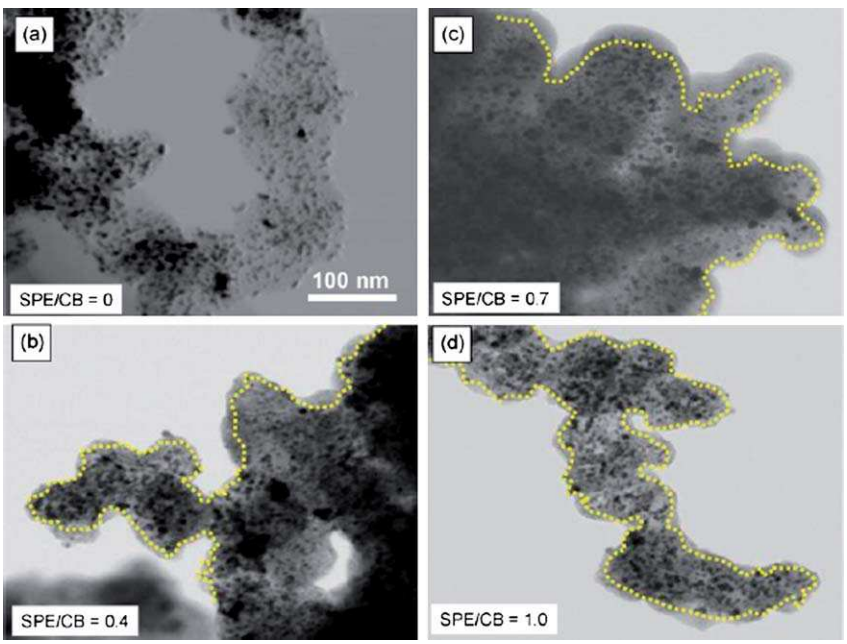

Fig. 4 Scanning transmission electron microscope (STEM) images of sulfonated polyether (SPE)-based catalyst layers (SPE IEC = 1.61 meq g^{-1}) for different SPE/carbon mass ratios.[113] Reprinted from Publication A. B. Beleke, K. Miyatake, H. Uchida and M. Watanabe, Gas diffusion electrodes containing sulfonated polyether ionomers for PEFCs, *Electrochim. Acta*, 2007, **53**, 1972. Copyright 2010, with permission from Elsevier.

revealed the presence of two types of micropores in Pt/C and Pt/C-ionomer. The authors distinguish secondary pores as being >50 nm, and report that catalyst layers containing sulfonated polyether exhibit a larger secondary-pore volume (pores > 50 nm) than uncoated Pt/C catalyst. By studying catalyst layers containing polymers possessing a range of IEC (0 to 4 meq g^{-1}) they found the maximum primary and secondary pore space is achieved using a sulfonated polyether of 2.17 meq g^{-1} and a polymer/carbon black ratio of 0.7 (25 wt% polymer in the CL). Moreover, they found that CLs possessing the highest porosities showed superior fuel cell performances.

Notwithstanding the possibility of localization of the polymer electrolyte at interfaces, as shown in Fig. 4, the proton conducting polymer is typically distributed homogeneously throughout the thickness of the catalyst layer, which ensures connectivity between aggregates of Pt/C and a continuous pathway for proton conduction between the membrane and catalyst reaction sites. However, it does not necessarily follow that the proton conductivity of the polymer in a catalyst layer is the same as that when cast as a membrane because in the former case it is distributed throughout a meso- and micro-porous carbon structure. The proton conductivity in a CL can be measured, *in situ*, in a fuel cell using electrochemical impedance spectroscopy (EIS), mathematical models incorporating electrical resistances in parallel with various capacitances are used to deconvolute the contributions of the different elements: namely, ion resistance of the CL and membrane, reaction kinetics, and mass transport parameters.[114,115] Diffusional processes associated with reactant mass transport occur on a much longer time scale to electrochemical charge transfer processes and hence their influences are revealed at different frequencies.[63,116] In fuel cell analyses, the influence of ionic transport and double layer charging of the electrode is often evident in the high frequency region (>1k Hz) of Nyquist plots. A straight line on a Nyquist plot having 45° slope may be observed in the high-frequency limit when operating the cell under N_2, so as to suppress electrochemical oxygen reduction. Under these conditions a linear feature corresponds to an electrode operating under the case of limiting proton transport. While readily observed under a wide range of operating conditions for PFSA-based CLs, in the case of polyaromatic-based CLs, the ionic resistance is often too large to accurately extract since the transition to the capacitive regime cannot be observed. Thus significant care and attention are required to extract information about the ionic conductivity of polyaromatic-based CLs and researchers often resort to devising methods utilizing *ex situ* conductivity analyses.

In order to extract the conductivity of the sulfonated hydrocarbons in a catalyst layer Ma *et al.*[71] examined sulfonated polyarylene ether sulfone (sPES), polyethersulfone post-sulfonated (sPES-PS), and Nafion® in CLs by evaluating the conductivity of agglomerates *ex situ* in "reactions layers" (Pt/C was replaced with alumina).[71] For both polyaromatics and perfluorinated polymers, the conductivities of the polymers were found to be two orders of magnitude lower than those measured for the same polymer in the form of a membrane. Moreover, between 20 °C and 100 °C, the proton conductivity of the Nafion®-based *reaction layer* was found to remain higher than sPES-PS based layers, and increased faster with temperature. The conductivity of sPES having a degree of sulfonation of 50% was found to be higher than that of Nafion® at 20 °C but lower above 60 °C.

Park *et al.*[56] and Peron *et al.*[61] attempted to establish a direct correlation between the porosity of a catalyst layer, electrochemical properties, and fuel cell performance. The former[56] calculated the porosity for 30 wt% sPEEK based CL (IEC 1.72 meq g^{-1}) to be similar to that of a 45 wt%-Nafion® based CL. Fuel cell performance curves of sPEEK-based MEAs prepared using the catalyst coated gas diffusion layer technique are reproduced in Fig. 5.[56]

The sPEEK loading in the cathode was varied from 10 to 40 wt%. The curves are characterized as exhibiting large overpotential losses under low current density, compared to PFSA–MEAs. The optimal sPEEK loading for highest fuel cell performances was found to be 30 wt%; *in situ* EIS measurements confirmed this loading to correspond to the lowest electrochemical charge transfer resistance for the ORR, which were 4.8, 2.6, 1.6 and 1.7 Ohm cm^{-2} for ionomer contents of 10, 20, 30 and 40%, respectively (measured under H_2/air at 75 °C, 100% RH). This decrease in resistance is attributed to an increase in conductivity for polymer contents between 10 and 30 wt%; the value obtained with 40 wt% sPEEK is attributed to a decrease in *electronic* conductivity due to coverage/blocking of carbon particles by the polymer.

Peron *et al.*[61] reported a lower optimal sPEEK content for catalyst layers (~20 wt%) but it should be noted that MEAs were prepared using the catalyst-coated membrane (CCM) technique and using a sPEEK polymer having a lower IEC (1.4 meq g^{-1}). EIS analyses revealed a large increase in proton conductivity of the catalyst layer when the polymer loading was >40 wt%—attributed to the threshold above which there is maximal

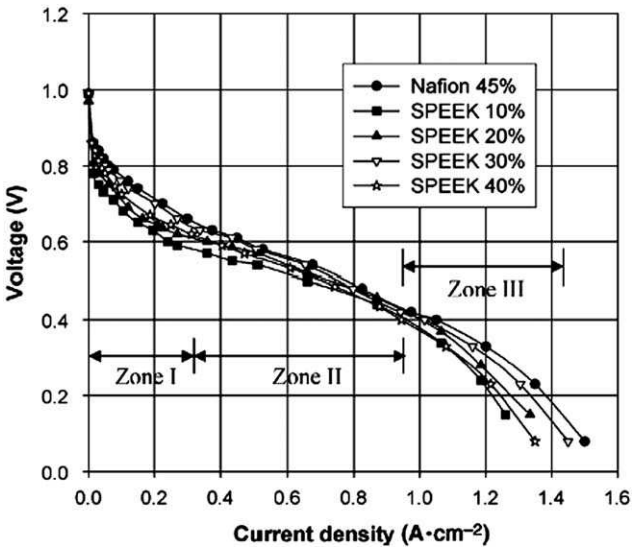

Fig. 5 Polarization curves for catalyst layers with different polymer contents (75 °C; H_2/air: 1.5/2, ambient pressure; 100/100% RH anode/cathode. Zone I: influence of charge transfer kinetics; Zone II: Ohmic resistance; Zone III: mass transport resistance.[56] Reprinted from Publication: J. S. Park, P. Krishnan, S. H. Park, G. G. Park, T. H. Yang, W. Y. Lee and C. S. Kim, A study on fabrication of sulfonated poly(ether ether ketone)-based membrane–electrode assemblies for polymer electrolyte membrane fuel cells, *J. Power Sources*, 2008, **178**, 642. Copyright 2010, with permission from Elsevier.

connectivity of the polymer aggregates throughout the CL. Poor fuel cell performances were observed for sPEEK loadings of 10 wt% and less, for which proton conductivity was insufficient, and 40 wt%, for which oxygen mass transport limitations dominated.

Reports on a catalyst layer based on a sPEEK–PTFE composite also report a dramatic increase in proton conductivity of the catalyst layer and severe limitations in oxygen mass transport when the CL contains >40 wt% of the polymer electrolyte.[63] EIS was used in a H_2/O_2 fuel cell to quantify the total ionic and electronic resistance, R_T, of the MEA, which includes the uncompensated resistance, R_u (membrane resistance, cell resistance, and cell hardware resistance). A typical Nyquist impedance response for 10 wt% sPEEK-based cathode catalyst layer under increasing current density is shown in Fig. 6.[63] The EIS arc response represents the combined magnitude of the charge transfer resistance, R_{CT}, and mass transfer resistance, R_{MT}, occurring in the cathode under H_2/O_2. At high current densities, the contribution due to charge transfer resistance is negligible. The transition from charge transfer to mass transport limitations is demonstrated by plotting the real resistance (Z') against current density, which is shown in Fig. 6 (right) for sPEEK-based cathodes containing different sPEEK contents.

The transition to the mass transfer controlled regime is indicated by the change in slope in Fig. 6 (left) at ~200 mA cm^{-2}. The highest loadings of sPEEK catalyst layers (30 and 40 wt%) show significantly larger mass transfer limitations than the lower weight content catalyst layers. This is illustrated by comparing the real resistance (Z') at the fixed current density of 350 mA cm^{-2} in Fig. 6 (right). This current density is representative of the mass transfer controlled regime of the polarization curve for each MEA, and it can be observed that the mass transport resistance increases linearly with increasing electrolyte content. Higher loadings of sPEEK electrolyte in the catalyst layer support higher proton conductivity values, but also result in stronger mass transport resistance. However, in this study, the maximum fuel cell performance was obtained for a polymer loading of 10 wt%.[57,63] The incorporation of hydrophobic PTFE as well as the much higher IEC (1.9 meq g^{-1}) may have limited the performance of catalyst layers prepared with higher polymer loadings, moreover, the fuel cell experiments were performed at 35 and 50 °C so that flooding of the catalyst layer may be significant, and also the catalyst layers were prepared by the catalyst coated membrane technique. Using a sPEEK sample having an IEC of 1.88 meq g^{-1}, half-cell experiments indicated that the maximum Pt utilization occurs for sPEEK loadings of 15 wt%.

In DMFC applications, Lee *et al.*[64] reported the optimum sPEEK loading in the cathode to be 20 and 25 wt%. At this loading, the electrochemical surface area (ESA) of Pt was at its highest while the interfacial resistance between the membrane and the polymer in the catalyst layer was at its lowest. In the case of sulfonated polyether containing (fluorenylidene biphenyl) groups SPE, Beleke *et al.*[113] varied the ionomer content from 0.4 to 1.0 I/C ratio. For a SPE having an IEC of 1.61 meq g^{-1}, the maximum performance was obtained for an I/C ratio of 1.0 (which translates to 33 wt% of the polymer in the CL). When the polymer content is maintained at 26 wt%, an SPE sample with an IEC of 2.17 meq g^{-1} provides the highest fuel cell performance, while polymers having an IEC of 1.61 and 3.17 meq g^{-1} yield a lower performance. This study highlights the strong role of the hydrophilicity and water uptake properties of the polymer and the importance of optimizing both the polymer's IEC and the polymer content in the CL.

Krishnan *et al.*[117] studied the fuel cell performances of MEAs prepared from sulfonated partially fluorinated (sF-PES) and sulfonated non-fluorinated poly(ethersulfone) (sPES), both as a membrane and incorporated into the catalyst layer. The IEC of sF-PES and sPES was 1.28 meq g^{-1} and 1.43 meq g^{-1}, respectively and the content in the CLs was varied from 1.5 to 32 wt%, and in both cases the optimal loading was of 2 wt%, which is exceptionally low. At 0.2 A cm^{-2}, the potentials of the cells were 0.56 V and 0.59 V, respectively for sF-PES and sPES, and the charge transfer resistances measured under H_2/O_2 at 0.85 V were 3.9 Ω cm^2 and 2.7 Ω cm^2. Despite the high proton conductivity measured (~0.09 S cm^{-1}) for membranes of the polymers at 100% RH, rt, the fuel cell performances were extremely low.

Muldoon *et al.*[78] studied the MEA fuel cell performances of cathode catalyst layers prepared with 5, 15 and 30 wt% of sulfonated polyphosphazene (1.58 meq g^{-1}). Despite the polymer exhibiting similar proton conductivities to and higher oxygen permeability than Nafion®, the optimal performance and highest electrochemical surface areas were obtained for a polymer content of 15 wt%, which confirms the necessity to examine other structural properties of the polymer that could account for differences in the optimum polymer content.

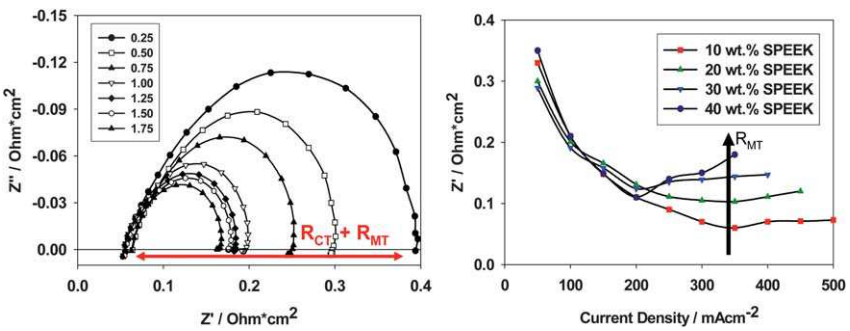

Fig. 6 EIS Nyquist response for SPEEK-based catalyst layers (10 wt% SPEEK) under increasing cell current. (Left) H_2/O_2 at 0.2 L min^{-1} and 50 °C cell temperature. (Right) Total ionic and electronic resistance of the CL for 10 (■), 20 (▲), 30 (▼), and 40 (●) wt% SPEEK contents.[63] Reproduced with permission from *J. Electrochem. Soc.*, 2009, **156**(4), B499. Copyright 2003, The Electrochemical Society.

Higuchi *et al.*[73] studied the influence of polyimide-based catalyst layers having polymer contents ranging from 10 to 40 wt%. When the ionomer loading was increased from 20 to 30%, the performance loss was >100 mV at 0.3 A cm^{-2}, and the mass activity significantly reduced from 15 to 3 A g^{-1}. The Tafel slope increased from 100 to 120 mV dec^{-1} when the polymer content was increased from 10 to 40 wt%. Thus higher performances and mass transport activity are observed for relatively low polymer loadings. However, the performance was much lower than those reported for Nafion®-based CLs, and this is attributed to lower oxygen permeation through the CL as well as a different, but undefined, distribution of polymer within and/or around the supported-catalyst particles. Similar to other studies on hydrocarbon polyelectrolytes increasing the polymer content to >30 wt% decreases the porosity of the catalyst layer and results in a concomitant loss of fuel cell performance.

Kim *et al.*[75] studied the impact of increasing the H_3PO_4/PBI content in the catalyst layer on MEAs prepared with 2,5-polybenzimidazole (AB-PBI) membranes. The loading determined for this H_3PO_4-doped polyheterocyclic system was found to be optimum at 20 wt%. At this value, the Ohmic resistance of the MEA was at its lowest, and is considered to provide an optimum balance between the ionic and electronic conductivities. Seland *et al.*[118] also examined the optimal H_3PO_4/PBI content for the *anode* catalyst layer. When the PBI loading was increased a noticeable increase in fuel cell performance was observed, increasing the polymer content further led to a drop of performance due to isolation and blocking of active catalyst particles. The optimal PBI loading was found to be 30 and 33 wt% for the anode and cathode catalyst layers, respectively.

For similar ionomer contents, it seems that the overall porosity of catalyst layers containing polyaromatic or polyheterocyclic ionomer is lower than Nafion®-based CLs. For low polymer contents in the catalyst layer, the proton conducting pathway is insufficient; for high contents, gas transport to reaction sites *and* electronic conductivity are impaired. The optimum range of ionomer loading, between too low and too high an ionomer content, is narrower than for Nafion®-based catalyst layers and is strongly dependent on the components and on the preparation conditions. It appears that the optimum loading for polyaromatic and polyheterocyclic ionomers is less than 30 wt% observed for Nafion®-based catalyst layers.

3.2 Influence of IEC

Sambandam and Ramani[58,59] and Ramani *et al.*[66] report the influence of the IEC on the properties of sulfonated polyetheretherketone (sPEEK)- and sulfonated polyetherketoneketone (sPEKK)-based CL properties and fuel cell performances. It is shown[59] that for a similar polymer content the ESA and ORR kinetics of the catalyst layer increase with increasing IEC of sPEEK (from 1.35 to 2.1 meq g^{-1}), while cathodic Ohmic and concentration overpotentials decrease. However, ESAs of sPEEK-based systems were more than 25% lower than those of Nafion®-based catalyst layers. In the case of sPEKK based-catalyst layers, notwithstanding the higher ESA values, lower fuel cell performances are observed for higher IEC polymers[55] which is attributed to larger contact resistances at the membrane–cathode interface arising from interfacial immiscibility. As is discussed later in this review, differences in IEC and water content of the polymer in the catalyst layer and in the membrane can induce incompatibility between the catalyst layer and the membrane. In this particular case, the high IEC (2.1 meq g^{-1}) might be responsible for the performance decrease. Indeed, as reported by Lee *et al.*[64] and Yoda *et al.*[70] high IEC polymers in catalyst layers may have a detrimental effect on performance due to an increased propensity to flooding, mass transport limitations, and catalyst poisoning due to the higher concentration of sulfonic acid groups. They also reported the influence of the IEC of sPEEK on the performances of catalyst layers in DMFC applications. For a loading of 20 wt%, they found the optimum IEC of the polymer in the catalyst layer to be 1.33 meq g^{-1}. Using MEAs prepared from catalyst slurry deposited on a GDL by brushing and subsequent hot-pressing onto Nafion® 115 membranes, they observed a performance drop from 0.3 V to 0.22 V at 0.1 A cm^{-2} when the IEC of the polymer was decreased from 1.51 to 1.33 meq g^{-1}. While no significant difference was observed in the kinetic region, the main differences arise from Ohmic and mass transport limitations. For the lowest IEC, the poor performance was attributed to a higher protonic resistance, for highest IEC the decrease in performance was attributed to mass transport losses and a decrease in permeability to reactant gases due to high water content. In the case of sulfonated poly(arylene ether) sPAE-CLs, Yoda *et al.*[70] reported a higher performance, lower Tafel slopes and larger Pt mass activity under lower relative humidity (RH) for sPAE—having 1.8 meq g^{-1}, compared to 2.5 meq g^{-1}. Between 60 and 78% RH, the higher performance obtained for lower IEC was attributed to lower sulfonic acid concentration in the CL, thus mitigating the specific adsorption of the ionomer at the Pt catalyst particles. The lowest Tafel slope and highest mass activity were observed for the 2.17 meq g^{-1} polymer[113] when comparing polymers in the catalyst layer with IECs having 1.63, 2.17 and 3.73 meq g^{-1}. As in the case of sulfonated polyetherketones, when sulfonated polyether is introduced in the catalyst layer the fuel cell performance increases up to a critical IEC value.

The range of IEC of sulfonated hydrocarbon ionomers that can be used in a fuel cell is limited because low IEC polymers possess insufficient proton conductivity and high IEC polymers are too hydrophilic. For a sufficient proton conductivity, IECs of polyaromatics usually have to be larger than that of Nafion®. At high relative humidity, excessive swelling of the sulfonated polyaromatics suppresses the permeation of oxygen gas and leads to instability of polarization curves. Polyaromatics often appear much more sensitive to RH than PFSAs. For all the polyaromatic ionomers presented here, under low RH proton conductivity drops dramatically as does the hydration number of the sulfonated ionomers.

3.3 Influence of dispersion media

As described in the Introduction the dispersion medium used in the preparation of the catalyst ink influences the properties of the resulting catalyst layer. Because the dispersion medium influences polymer–polymer, polymer–Pt/C, Pt/C–Pt/C interactions the effect of a particular dispersion medium is expected to be specific to a particular polymer. In the context of hydrocarbon

polyelectrolytes, the information on the influence of the catalyst dispersion medium is extremely sparse. Sung *et al.*[60] have shown using dynamic light scattering that commercial Nafion® *dispersions* in alcohol have a rather broad particle distribution with a mean diameter ~200 nm. In contrast sPEEK in dimethylacetamide (DMAc) forms particles of size ~10 nm. Unlike PFSA, dissolution of polyaromatic polyelectrolytes requires aprotic solvents of high dielectric constant, such as dimethylacetamide (DMAc), *N*-methylpyrrolidone (NMP), dimethyl sulfoxide (DMSO), dimethylformamide (DMF). Such solvents lead to a complete solvation of polymer chains and the formation of a true "polymer solution", which will impact catalyst layer formation.[119–121] Sung *et al.*[122] have shown that the porosity of sPEEK-based catalyst layers, determined by Hg porosimetry, depends on the solvent choice for solution preparation. DMAc or DMF-based catalyst inks led to catalyst layers exhibiting larger pores and a higher overall porosity compared to NMP and DMSO-based inks. These structural characteristics were shown to have a direct impact on the gas permeability and on performances of the cathodes prepared for DMFC applications, particularly in the mass transport limited region. Von Kraemer *et al.*[68] also studied the influence of different solvent systems on the porosity of sulfonated polysulfone (SPSU)-based catalyst layers, comparing the following systems: 2-propanol/water, acetone/water, and DMAc. The lowest BET surface area and the lowest primary pore volume (pores < 10 nm) were obtained for catalyst layers prepared from DMAc solutions and were found to be 35 $m^2 g^{-1}$ and 7 $m^2 g^{-1}$, respectively *vs.* 42 $m^2 g^{-1}$ and 13 $m^2 g^{-1}$ for catalyst layers prepared either from 2-propanol/water or acetone/water mixture. This observation is attributed to a better solubilization of the polymer in DMAc, allowing for a higher coverage of the Pt/C particles. As proposed by Sung *et al.*,[122] this phenomenon is due to the difference in the solvent's boiling point—the higher boiling point leading to a slower evaporation and a reduced porosity.

The interaction of the proton conducting polymer with catalyst particles is expected to be influenced by the solvent. Highly polar solvents, and solvents possessing benzene/phenyl rings or benzimidazole heterocycles are suspected of interacting with Pt, thus suppressing electrochemical activity—the poisoning of Pt by imidazole has been reported.[123] Moreover, Sung *et al.*[122] report that sPEEK when cast from DMF, as opposed to DMAc, resulted in increased CL resistances, as measured by EIS, and was attributed to interactions between sPEEK and the solvent. Sambandam and Ramani[58] also reported a 30% decrease in Pt electrochemical surface area when Nafion®-based inks are prepared from DMAc instead of alcohols. Given the limited reports in this area, and the fact that the ink dispersion medium alone can influence the performance of catalyst layers, irrespective of the nature of the polymer, means this highly critical area remains unclear and warrants further attention.

3.4 Introduction of additives or porogens

Different strategies have been considered to enhance gas and water transport in catalyst layers that incorporate hydrocarbon polylectrolytes. Astill *et al.*[63] studied the incorporation of hydrophobic polytetrafluorethylene (PTFE) in sPEEK-based CLs with the aim of improving water management. The main pore size in sPEEK/PTFE-based catalyst layers was larger than in Nafion®-based systems; however, the overall CL porosity was lower and no improvement in performance was observed. Pan *et al.*[77] studied the influence of the introduction of porogens in PBI catalyst layers. By introducing 4 wt% of ammonia oxalate into the catalyst slurry, the porosity of the catalyst layer was increased to 62% from 42–44%. By using ZnO, the porosity was increased to 60%, and when ammonium carbonate or ammonium acetate was used, the porosity was >50%. A larger porosity enhances the cathodic and anodic limiting current densities and utilization of hydrogen. Removal of the ammonium salts to form pores, performed at elevated temperature, leads to the formation of cracks or larger pores that facilitated gas transport. Kim *et al.*[62] reported the utilization of polyethylene glycol (PEG) as a porogen to form porous sPEEK-based CLs. CLs prepared from sPEEK/PEG possess larger pore volume, broader pore size distribution, and larger BET surface areas (15.2 $m^2 g^{-1}$ *vs.* 9.3 $m^2 g^{-1}$) compared to regular sPEEK-based CLs. The PEG is found to mainly influence the volume of the secondary pores (>50 nm).

3.5 Durability

The durability of hydrocarbon polyelectrolytes, particularly at elevated temperature, is an area of grave concern. Several groups have attempted to determine degradation mechanisms of various polymer membranes at elevated temperature and under oxidative environments. The glass transition and decomposition temperatures of their sulfonated derivatives are generally >150 °C;[124,125] however their chemical and thermomechanical stability remains problematic. Mechanical degradation of membranes in fuel cells results from swelling and deswelling cycles, pressure of gases. The Fenton's test using a H_2O_2 solution containing a trace amount of Fe^{2+} has become a common *ex situ* accelerated method for evaluating membranes stability to oxidative conditions. Typical peroxide concentrations used to determine PFSA-membrane stability are 3% or 30%, which are much higher than those encountered in fuel cells. As reported by LaConti *et al.*[126] the stability of non-perfluorinated polymers studied *ex situ* in Fenton's oxidative conditions is generally much lower than that of Nafion®. The harsh conditions usually used to evaluate the stability of PFSA membranes are too harsh for polyaromatic polymers and their degradation occurs too rapidly to isolate degradation intermediates and to provide an understanding of degradation mechanisms. Milder conditions, using lower concentration of H_2O_2 and Fe^{2+}, appear to be more relevant to simulate the degradation of polyaromatic polymers in the presence of hydroxy or peroxy radicals. Membranes investigated in this manner include: sulfonated polyetheretherketones,[127] sulfonated polyaryletherketones,[128] sulfonated polysulfones,[124] polyarylethersulfones,[129] poly(styrenesulfonic acid)-grafted polyetheretherketone,[130] biphenylsulfone hydrocarbons[131] and polybenzimidazoles.[132] After several hours in H_2O_2 or H_2O_2/Fe^{2+}, polyaromatic and polyheterocyclic membranes often become brittle, their surface is damaged, they lose mass and exhibit reduced mechanical strength due to a decrease in polymer molecular weight.[128,129,132–134] Despite various studies being carried out on the synthesis and durability of sulfonated hydrocarbon-based polymers their mechanism of degradation is

still not clearly understood. Using EPR, Hubner and Roduner[135] studied the degradation of model compounds in the presence of radicals generated by the photolysis of H_2O_2. The dominant degradation pathway is the addition of $HO^{\bullet}$ to the aromatic ring, usually ortho to the alkyl- or RO-substituent. Studying the degradation of sulfonated aryletherketone in H_2O_2, Perrot *et al.*[127] found that ether linkages are much more sensitive to oxidation than ketone linkages. Their degradation leads to polymer chain scission and the formation of both carboxylic and phenol end chains. After ageing sPAEK membranes in H_2O_2, Perrot *et al.*[128] used IR spectroscopy to detect carboxylated products in eluted water but not in the aged membrane material. From these results, the authors favor a degradation mechanism originating from chains ends. While main chain scission should allow accumulation of carboxylated species in the membrane, degradation through an unzipping mechanism favors the elution of small carboxylated species. Studying sulfonated polyethersulfones, Lawrence and Yamaguchi[129] found that sPES copolymerized with 4,4′-biphenylsulfone was more stable towards oxidative attack than sPES copolymerized with 4,4′-benzophenone; degradation of the former mainly occurred by an edge scission mechanism and degradation of the latter occurred by both edge-scission and main chain scission mechanisms. From their study, they concluded that utilization of a combination of functional groups imparting steric hindrance and strong electronegativity was likely to increase the durability of sulfonated polyaromatics. Studying the degradation of PBI in Fenton's solution, Chang *et al.*[132] proposed a degradation mechanism in which the N–H bond of the imidazole ring was susceptible to be oxidized, and the benzene rings were oxidized to quinine and dicarboxylic acid structures. Li *et al.*[136] demonstrated that the presence of strongly electron withdrawing groups introduced into polybenzimidazoles increases their oxidative stability; indeed radicals predominantly attack electron-rich aromatic compounds.[136] After the Fenton test, a bimodal molecular weight distribution curve was obtained for polybenzimidazoles containing $–SO_2–$ and $–C(CF_3)_2–$ functional groups, which suggest a midpoint chain scission mechanism, while a monomodal molecular weight distribution was obtained in the case of pure PBI which is indicative of a degradation mechanism starting from the chain ends.[136] While electron withdrawing groups decrease the electron density of the adjacent aromatic rings and thus decrease their sensitivity towards radicals attack, the introduction of heteroatom groups confers an additional weakness. The formation of blend membranes, and thus physical interaction between polymer chains, is another way that has been shown to preserve membrane integrity by limiting the elution of low molecular weight compounds resulting from the degradation. Vogel *et al.* used electron paramagnetic resonance to study the degradation of sulfonated polyetheretherketone and sulfonated poly(phthalazinone ether ketone) in contact with gaseous hydrogen peroxide, and found the latter to be more stable toward hydroxyl radicals than sPEEK.[137] While perfluorinated ionomers are stable toward hydrolysis, other polymers such as polyimides are less stable in water.[138] Determination of polymer degradation mechanisms *ex situ* is preferred to studies performed on a fuel cell because the former limits the number of factors that can influence degradation. However, the degradation path is strongly depending on experimental conditions, and this has limited our understanding of polymer degradation. This topic is of high importance in the design of new polymer structures.

The second issue concerning the durability of catalyst layers and MEAs prepared using hydrocarbon polyelectrolytes is miscibility. Relatively few polymers are miscible with other polymers. Even polymers possessing a similar backbone but prepared with a different ion exchange capacity may be immiscible in the solid state. This phenomenon has been reported by Ramani *et al.*,[66] wherein a mixture of two polymer solutions of sulfonated polyetherketoneketone (sPEKK) of different IEC leads to phase separation in the resulting cast membrane. Similarly, using polymers of similar structure but with different IEC in the catalyst layer and membrane respectively may lead to a non-adhering interface. Ramani *et al.*[66] have attributed the lower performances of higher IEC sPEKK-based CL to this lack of compatibility. This point represents a major limitation when considering the use of polyaromatic ionomers in fuel cells. Polyaromatic polymers are usually functionalized directly in conc. sulfuric acid, which may represent an advantage in scaling-up the synthesis. However, even under similar reaction conditions the degree of sulfonation of polyaromatic polymers can vary widely between synthetic batches. Sulfonated polyetheretherketone (sPEEK)[53] and sulfonated polyarylsulfones (sPAES)[52] have been incorporated in catalyst layers and examined in methanol fuel cells, and while the beginning-of-life performances of sPEEK[53] or sPAES[52]-based MEAs were lower than MEAs prepared with polyaromatic membrane and Nafion®-based catalyst layer, the interfacial resistance of the catalyst layer/membrane interface remained constant during operation, whereas that of the Nafion®/polyaromatic–MEA increased significantly. The lack of compatibility between the polyaromatic electrolytes and perfluorosulfonic leads rapidly to delamination of the CL from the membrane and a decrease in fuel performance. Similarly, Lee *et al.*[64] reported improved performances, and notably lower interfacial resistances of MEAs comprised of sPEEK in the membrane *and* catalyst layers, compared with using dissimilar polymers. In order to improve compatibility between polyimide membranes and Nafion®-based catalyst layers and to enhance interfacial stability, Sung *et al.*[72] studied the incorporation of a crosslinkable layer at the membrane/catalyst layer interface. In DMFC, the initial performance of the MEA containing crosslinked poly(ethylene glycol) dimethacrylate (PEGDMA) shows lower performance and lower ESA; however such MEAs show lower methanol crossover, and the dense and continuous interface between the membrane and the electrode was maintained after long term operation.

During the past few years much effort has gone into elucidating degradation mechanisms of Nafion®-based MEAs under various conditions of operation. It is now well known that oxidized Pt species produced under high potentials can migrate in PFSA membranes. The presence of oxidized Pt species throughout the MEA appears responsible for increasing the rate of peroxide radical formation and PFSA membrane degradation.[34,36,139,140] While Pt migration has also been reported in phosphoric acid–polybenzimidazole MEAs,[141] OCV experiments performed on MEAs prepared with sPEEK membranes and Nafion®-based CLs have shown that Pt does not migrate into polyaromatic electrolytes.[142] In Nafion®-based CLs a distinct

decrease in the thickness of the cathode CL has been observed, however the platinum surface density was found to be equal at the anode and cathode. No Pt was seen or detected in the polyaromatic membrane distant from the electrodes, however particles were observed close to the electrodes. Two main reasons could account for the difference in degradation mechanisms which might explain why Pt is not observed in the membrane when the ionomer and the polymer that form the membrane are different: incompatibility between the coordination sphere of oxidized Pt species that results from ionomer degradation, and the membrane electrolyte, which might be responsible for Pt re-precipitation in the cathode CL. The non-migration of Pt species into polyaromatic electrolyte could also be explained by the polymer structure being of lower acidity and the reduced propensity of the polymer to facilitate oxidation of Pt.

4. Conclusions and perspectives

While the types of sulfonated hydrocarbon polymers studied have been quite varied, as have the conditions and compositions of the catalyst inks and catalyst layers, trends are emerging regarding the incorporation of sulfonated hydrocarbon polymer in catalyst layers. For example, whereas two types of pores can be distinguished in Nafion®-based CLs, sPEEK-based catalyst layers often exhibit mono-modal pore size distributions, typically centered at ~50 nm.[60,61] While the pores size distribution is bigger the overall porosity is lower than Nafion®-based CLs. These differences may be related to the polymer : Pt/C interactions present in the catalyst ink. Polyaromatic or polyheterocyclic polymers tend to dissolve, forming true solutions, whereas PFSA ionomer is used in its colloidal state. Single chains in solution may penetrate and block primary pore space, or coat individual Pt/C particles thus interfering with the agglomeration of Pt/C particles which produce primary pores. The intimate presence of sulfonated polymers in the primary pore space may affect the transport of gases to the catalyst particles and impede the egress of product water. Moreover, lack of aggregation and an ionic network caused by strong interactions of the polymer with the catalyst particles may lead to poor proton conduction throughout the polymer phase. Another issue is that in the preparation of catalyst inks sulfonated polyaromatics generally require the use of strongly polar aprotic solvents with high boiling points. Excessive thermal or chemical post-treatment may be required to completely remove residual solvents, which affects the CL structure.

Increasing the sulfonated hydrocarbon polymer content in a catalyst layer decreases the porosity and impairs gas diffusion, and also decreases the connectivity of the catalyst/carbon network so as to reduce the electronic conductivity of the catalyst layer. Electrochemical kinetics of the ORR in the low current regime depends on wetting of the Pt catalyst by the hydrophilic domains determined by the solid polymer electrolyte, the ability of the CL to support proton transport, and the quality of the connectivity and electronic conductivity of the carbon particles in the cathode. As with PFSA-based CLs, there is an optimum content for sulfonated polyaromatic polymers. For low polymer contents in the catalyst layer, the proton conducting pathway will be insufficiently developed; for high contents, gas transport to reaction sites *and* electronic conductivity will be impaired. The apparent stronger interaction between the hydrocarbon polymer chains and Pt/C particles leads to densification of the CLs, even for low polymer loadings, which suppresses the fuel cell performance. It would appear that the optimum loading is lower than the 30 wt% observed for Nafion®-based catalyst layers. Different strategies have been considered to improve the porosity of sulfonated polyaromatic-based CLs, such as the introduction of porogens.[62,77] These appear to improve the mass transport without impeding the catalytic activity but the presence of large pores does not enhance ORR kinetics nor proton transport.

Gas permeability of sulfonated polyaromatics is usually much lower than PFSAs, by a wide margin. While this is a positive attribute when the polymer is employed as the membrane, it may be detrimental when employed in a catalyst layer because of its impact on ORR kinetics. Gas permeability is strongly dependent on the water content of the polymer, and hence on the ion exchange capacity. The higher the degree of sulfonation, the higher the water uptake, the higher the gas permeability. However, highly sulfonated polymers sorb, and desorb, large amounts of water which invoke large dimensional changes which can affect the membrane's mechanical stability when subjected to the large variations in RH and temperature found during typical fuel cell operation. Moreover, highly sulfonated, high water-containing polymers in catalyst layers show a stronger propensity for flooding, which impedes gas transport. Reducing the polymer content in the CL for high IEC polymers may be an acceptable strategy when sufficient water is present but the same catalyst layer system under low RH will suffer from poor protonic conductivity as the hydration number of the sulfonated drops dramatically. The negative influence of reducing the RH has been confirmed by studies using sPEEK[61] and SPAE.[69] At high relative humidity, excessive swelling of the sulfonated polyaromatic suppresses the oxygen gas diffusion[69] and leads to instability of polarization curves.[61] The issue of RH dependence on fuel cell performances is exacerbated in sulfonated polyaromatics because the water contents in the polymer, at IECs that are useful for fuel cells, often appear much more sensitive to RH than PFSAs. These represent significant challenges when considering new proton conducting polymers for fuel cell systems.

It is recommended that future investigations into sulfonated polyaromatic membranes be directed to structures that promote phase separation of the polymer into more distinct hydrophobic and hydrophilic domains, with the added variability of inducing aggregation of hydrophobic domains in a colloidal fashion that is observed for PFSAs. Several strategies are being considered for this including those that make use of block copolymers or graft copolymers to facilitate the formation of proton conduction channels.[143,144] To date these efforts have been directed to the study of new membranes but it is equally relevant to the fabrication of sulfonated polyaromatic-based CLs. Even in the case of perfluorinated ionomers such as Nafion®, the interaction of the individual polymer chains, and aggregates of polymer chains, with Pt/C in the catalyst ink and in the catalyst layer is poorly understood. The information that is known is derived from the simulation/modelling studies reported by Malek *et al.*,[121] which reveal that, in the case of Nafion®, the main chain adsorbs to surfaces of carbon agglomerates particles, while the side chains strive to maximize their separation on the agglomerate surface.

The ether-linked side chains, acid groups, hydronium ions and water molecules form interconnected hydrophilic clusters. Such studies applied to sulfonated polyaromatic would serve as a basis for the design of new proton conducting polymers. A complementary strategy to improve the performance of sulfonated polyaromatic based-CLs would be to develop catalyst supports that modify the interaction of the polymer with the support. In this context, the study of well-defined architectures based on nano-templated and random nanoporous electrodes deserves special attention.[145]

References

1 K. Epping Martin and J. P. Kopasz, *Fuel Cells (Weinheim, Ger.)*, 2009, **9**, 356.
2 K. Kinoshita, *Electrochemical Oxygen Technology*, John Wiley & Sons, NewYork, 1992.
3 K. C. Neyerlin, W. Gu, J. Jorne and H. A. Gasteiger, *J. Electrochem. Soc.*, 2006, **153**, A1955.
4 H. A. Gasteiger, S. S. Kocha, B. Sompalli and F. T. Wagner, *Appl. Catal., B*, 2005, **56**, 9.
5 S. Gottesfeld, *ECS Trans.*, 2008, **6**, 51.
6 M. Eikerling, A. A. Kornyshev and A. R. Kucernak, *Phys. Today*, 2006, **59**, 38.
7 P. Costamagna and S. Srinivasan, *J. Power Sources*, 2001, **102**, 242.
8 I. D. Raistrick, *US Pat.*, 4876115, 1989.
9 E. A. Ticianelli, C. R. Derouin, A. Redondo and S. Srinivasan, *J. Electrochem. Soc.*, 1988, **135**, 2209.
10 M. S. Wilson and S. Gottesfeld, *J. Appl. Electrochem.*, 1992, **22**, 1.
11 M. S. Wilson and S. Gottesfeld, *J. Electrochem. Soc.*, 1992, **139**, L28.
12 S. Litster and G. McLean, *J. Power Sources*, 2004, **130**, 61.
13 E. Antolini, *J. Appl. Electrochem.*, 2004, **34**, 563.
14 N. Garland, *Abstract: Advances in Materials for Proton Exchange Membrane Fuel Cell Systems*, Pacific Grove, CA, Feb 18–23, 2007.
15 D. L. Ho, J. P. Kopasz, T. G. Benjamin and W. F. Podolski, *Prepr. Symp. - Am. Chem. Soc., Div. Fuel Chem.*, 2009, **54**, 579.
16 S. Srinivasan, E. A. Ticianelli, C. R. Derouin and A. Redondo, *J. Power Sources*, 1988, **22**, 359.
17 M. Uchida, Y. Aoyama, N. Eda and A. Ohita, *J. Electrochem. Soc.*, 1995, **142**, 463.
18 M. Uchida, Y. Aoyama, N. Eda and A. Ohta, *J. Electrochem. Soc.*, 1995, **142**, 4143.
19 M. Uchida, Y. Fukuoka, Y. Sugawara, N. Eda and A. Ohta, *J. Electrochem. Soc.*, 1996, **143**, 2245.
20 E. Passalacqua, F. Lufrano, G. Squadrito, A. Patti and L. Giorgi, *Electrochim. Acta*, 2001, **46**, 799.
21 E. Antolini, L. Giorgi, A. Pozio and E. Passalacqua, *J. Power Sources*, 1999, **77**, 136.
22 K. A. Mauritz and R. B. Moore, *Chem. Rev. (Washington, DC, U. S.)*, 2004, **104**, 4535.
23 S. Wang, G. Sun, Z. Wu and Q. Xin, *J. Power Sources*, 2007, **165**, 128.
24 M. Watanabe, M. Tomikawa and S. Motoo, *J. Electroanal. Chem. Interfacial Electrochem.*, 1985, **195**, 81.
25 M. Uchida, Y. Fukuoka, Y. Sugawara, H. Ohara and A. Ohta, *J. Electrochem. Soc.*, 1998, **145**, 3708.
26 T. Soboleva, X. Zhao, K. Malek, Z. Xie, T. Navessin and S. Holdcroft, *ACS Appl. Mater. Interfaces*, 2010, **2**, 375.
27 M. Eikerling, A. S. Ioselevich and A. A. Kornyshev, *Fuel Cells (Weinheim, Ger.)*, 2004, **4**, 131.
28 Y. Sone, P. Ekdunge and D. Simonsson, *J. Electrochem. Soc.*, 1996, **143**, 1254.
29 G. Gebel, *Polymer*, 2000, **41**, 5829.
30 E. J. Roche, M. Pineri, R. Duplessix and A. M. Levelut, *J. Polym. Sci., Polym. Phys. Ed.*, 1981, **19**, 1.
31 W. Y. Hsu and T. D. Gierke, *J. Membr. Sci.*, 1983, **13**, 307.
32 Z. Siroma, N. Fujiwara, T. Ioroi, S. Yamazaki, K. Yasuda and Y. Miyazaki, *J. Power Sources*, 2004, **126**, 41.
33 P. J. Ferreira, G. J. la O', Y. Shao-Horn, D. Morgan, R. Makharia, S. Kocha and H. A. Gasteiger, *J. Electrochem. Soc.*, 2005, **152**, A2256.
34 R. Borup, J. Meyers, B. Pivovar, Y. S. Kim, R. Mukundan, N. Garland, D. Myers, M. Wilson, F. Garzon, D. Wood, P. Zelenay, K. More, K. Stroh, T. Zawodzinski, J. Boncella, J. E. McGrath, M. Inaba, K. Miyatake, M. Hori, K. Ota, Z. Ogumi, S. Miyata, A. Nishikata, Z. Siroma, Y. Uchimoto, K. Yasuda, K.-i. Kimijima and N. Iwashita, *Chem. Rev. (Washington, DC, U. S.)*, 2007, **107**, 3904.
35 J. Healy, C. Hayden, T. Xie, K. Olson, R. Waldo, M. Brundage, H. Gasteiger and J. Abbott, *Fuel Cells (Weinheim, Ger.)*, 2005, **5**, 302.
36 J. Peron, Y. Nedellec, D. J. Jones and J. Roziere, *J. Power Sources*, 2008, **185**, 1209.
37 L. Merlo, A. Ghielmi, L. Cirillo, M. Gebert and V. Arcella, *J. Power Sources*, 2007, **171**, 140.
38 L. Merlo, A. Ghielmi, L. Cirillo, M. Gebert and V. Arcella, *Sep. Sci. Technol.*, 2007, **42**, 2891.
39 K. D. Kreuer, M. Schuster, B. Obliers, O. Diat, U. Traub, A. Fuchs, U. Klock, S. J. Paddison and J. Maier, *J. Power Sources*, 2008, **178**, 499.
40 A. Ghielmi, P. Vaccarono, C. Troglia and V. Arcella, *J. Power Sources*, 2005, **145**, 108.
41 J. Peron, D. Edwards, M. Haldane, X. Luo, Y. Zhang, S. Holdcroft and Z. Shi, *J. Membr. Sci.*, 2011, **196**, 179.
42 S. Xue and G. Yin, *Eur. Polym. J.*, 2006, **42**, 776.
43 K. D. Kreuer, *J. Membr. Sci.*, 2001, **185**, 29.
44 R. W. Kopitzke, C. A. Linkous, H. R. Anderson and G. L. Nelson, *J. Electrochem. Soc.*, 2000, **147**, 1677.
45 Q. Li, R. He, J. O. Jensen and N. J. Bjerrum, *Fuel Cells (Weinheim, Ger.)*, 2004, **4**, 147.
46 J. Roziere and D. J. Jones, *Annu. Rev. Mater. Res.*, 2003, **33**, 503.
47 M. A. Hickner, H. Ghassemi, Y. S. Kim, B. R. Einsla and J. E. McGrath, *Chem. Rev. (Washington, DC, U. S.)*, 2004, **104**, 4587.
48 G. Maier and J. Meier-Haack, *Adv. Polym. Sci.*, 2008, **216**, 1.
49 Q. Li, J. O. Jensen, R. F. Savinell and N. J. Bjerrum, *Prog. Polym. Sci.*, 2009, **34**, 449.
50 D. J. Jones and J. Roziere, *Adv. Polym. Sci.*, 2008, **215**, 219.
51 Q. F. Li, R. H. He, J. O. Jensen and N. J. Bjerrum, *Chem. Mater.*, 2003, **15**, 4896.
52 H. Y. Jung, K. Y. Cho, K. A. Sung, W. K. Kim, M. Kurkuri and J. K. Park, *Electrochim. Acta*, 2007, **52**, 4916.
53 H. Y. Jung, K. Y. Cho, K. A. Sung, W. K. Kim and J. K. Park, *J. Power Sources*, 2006, **163**, 56.
54 Y. Y. Shao, G. P. Yin, Z. B. Wang and Y. Z. Gao, *J. Power Sources*, 2007, **167**, 235.
55 Z. Xie, X. Zhao, M. Adachi, Z. Shi, T. Mashio, A. Ohma, K. Shinohara, S. Holdcroft and T. Navessin, *Energy Environ. Sci.*, 2008, **1**, 184.
56 J. S. Park, P. Krishnan, S. H. Park, G. G. Park, T. H. Yang, W. Y. Lee and C. S. Kim, *J. Power Sources*, 2008, **178**, 642.
57 E. B. Easton, T. D. Astill and S. Holdcroft, *J. Electrochem. Soc.*, 2005, **152**, A752.
58 S. Sambandam and V. Ramani, *ECS Trans.*, 2007, **11**, 105.
59 S. Sambandam and V. Ramani, *Electrochim. Acta*, 2008, **53**, 6328.
60 K. A. Sung, W. K. Kim, K. H. Oh and J. K. Park, *Electrochim. Acta*, 2009, **54**, 3446.
61 J. Peron, D. Edwards, A. Besson, Z. Q. Shi and S. Holdcroft, *J. Electrochem. Soc.*, 2010, **157**, B1230.
62 W. K. Kim, K. A. Sung, K. H. Oh, M. J. Choo, K. Y. Cho, K. Y. Cho and J. K. Park, *Electrochem. Commun.*, 2009, **11**, 1714.
63 T. Astill, Z. Xie, Z. Shi, T. Navessin and S. Holdcroft, *J. Electrochem. Soc.*, 2009, **156**, B499.
64 J. K. Lee, W. Li and A. Manthiram, *J. Power Sources*, 2008, **180**, 56.
65 J. K. Lee, W. Li, A. Manthiram and M. D. Guiver, *J. Electrochem. Soc.*, 2009, **156**, B46.
66 V. Ramani, S. Swier, M. T. Shaw, R. A. Weiss, H. R. Kunz and J. M. Fenton, *J. Electrochem. Soc.*, 2008, **155**, B532.
67 S. von Kraemer, G. Lindbergh, B. Lafitte, M. Puchner and P. Jannasch, *J. Electrochem. Soc.*, 2008, **155**, B1001.
68 S. von Kraemer, M. Puchner, P. Jannasch, A. Lundblad and G. Lindbergh, *J. Electrochem. Soc.*, 2006, **153**, A2077.
69 T. Yoda, T. Shimura, B. Bae, K. Miyatake, M. Uchida, H. Uchida and M. Watanabe, *Electrochim. Acta*, 2009, **54**, 4328.
70 T. Yoda, T. Shimura, B. Bae, K. Miyatake, M. Uchida, H. Uchida and M. Watanabe, *Electrochim. Acta*, 2010, **55**, 3464.
71 C. Ma, L. Zhang, S. Mukerjee, D. Ofer and B. Nair, *J. Membr. Sci.*, 2003, **219**, 123.

72 K. A. Sung, K. Y. Cho, W. K. Kim and J. K. Park, *Electrochim. Acta*, 2010, **55**, 995.
73 E. Higuchi, K. Okamoto, K. Miyatake, H. Uchida and M. Watanabe, *Res. Chem. Intermed.*, 2006, **32**, 533.
74 J. H. Kim, H. J. Kim, T. H. Lim and H. I. Lee, *J. Power Sources*, 2007, **170**, 275.
75 H. J. Kim, S. J. An, J. Y. Kim, K. M. Jin, S. Y. Cho, Y. C. Eun, H. K. Yoon, Y. Park, H. J. Kweon and E. M. Shin, *Macromol. Rapid Commun.*, 2004, **25**, 1410.
76 A. Verma and K. Scott, *J. Solid State Electrochem.*, 2010, **14**, 213.
77 C. Pan, Q. Li, J. O. Jensen, R. He, L. N. Cleemann, M. S. Nilsson, N. J. Bjerrum and Q. Zeng, *J. Power Sources*, 2007, **172**, 278.
78 J. Muldoon, J. Lin, R. Wycisk, N. Takeuchi, H. Hamaguchi, T. Saito, K. Hase, F. Stewart and P. Pintauro, *Fuel Cells (Weinheim, Ger.)*, 2009, **9**, 518.
79 L. Zhang, C. Ma and S. Mukerjee, *Electrochim. Acta*, 2003, **48**, 1845.
80 T. Astill, PhD thesis, Simon Fraser University, Canada, 2008.
81 K. Miyatake, T. Omata, D. A. Tryk, H. Uchida and M. Watanabe, *J. Phys. Chem. C*, 2009, **113**, 7772.
82 Z. Liu, J. S. Wainright, M. H. Litt and R. F. Savinell, *Electrochim. Acta*, 2006, **51**, 3914.
83 Z. Liu, J. S. Wainright and R. F. Savinell, *Chem. Eng. Sci.*, 2004, **59**, 4833.
84 A. Ohma, S. Suga, S. Yamamoto and K. Shinohara, *J. Electrochem. Soc.*, 2007, **154**, B757.
85 T. Sakai, H. Takenaka and E. Torikai, *J. Electrochem. Soc.*, 1986, **133**, 88.
86 T. Sakai, H. Takenaka, N. Wakabayashi, Y. Kawami and E. Torikai, *J. Electrochem. Soc.*, 1985, **132**, 1328.
87 Z. Ogumi, T. Kuroe and Z. Takehara, *J. Electrochem. Soc.*, 1985, **132**, 2601.
88 Z. Ogumi, Z. Takehara and S. Yoshizawa, *J. Electrochem. Soc.*, 1984, **131**, 769.
89 F. N. Buechi, M. Wakizoe and S. Srinivasan, *J. Electrochem. Soc.*, 1996, **143**, 927.
90 S. S. Kocha, J. D. Yang and J. S. Yi, *AIChE J.*, 2006, **52**, 1916.
91 V. A. Sethuraman, S. Khan, J. S. Jur, A. T. Haug and J. W. Weidner, *Electrochim. Acta*, 2009, **54**, 6850.
92 N. Asano, M. Aoki, S. Suzuki, K. Miyatake, H. Uchida and M. Watanabe, *J. Am. Chem. Soc.*, 2006, **128**, 1762.
93 J. Saito, K. Miyatake and M. Watanabe, *Macromolecules*, 2008, **41**, 2415.
94 T. Shimura, K. Miyatake and M. Watanabe, *Eur. Polym. J.*, 2008, **44**, 4054.
95 E. Fontananova, F. Trotta, J. C. Jansen and E. Drioli, *J. Membr. Sci.*, 2010, **348**, 326.
96 R. He, Q. Li, A. Bach, J. O. Jensen and N. J. Bjerrum, *J. Membr. Sci.*, 2006, **277**, 38.
97 S. C. Kumbharkar, P. B. Karadkar and U. K. Kharul, *J. Membr. Sci.*, 2006, **286**, 161.
98 A. Parthasarathy, C. R. Martin and S. Srinivasan, *J. Electrochem. Soc.*, 1991, **138**, 916.
99 A. Parthasarathy, S. Srinivasan and A. J. Appleby, *J. Electrochem. Soc.*, 1992, **139**, 2530.
100 A. Parthasarathy, S. Srinivasan, A. J. Appleby and C. R. Martin, *J. Electrochem. Soc.*, 1992, **139**, 2856.
101 V. I. Basura, C. Chuy, P. D. Beattie and S. Holdcroft, *J. Electroanal. Chem.*, 2001, **501**, 77.
102 V. I. Basura, P. D. Beattie and S. Holdcroft, *J. Electroanal. Chem.*, 1998, **458**, 1.
103 P. D. Beattie, V. I. Basura and S. Holdcroft, *J. Electroanal. Chem.*, 1999, **468**, 180.
104 L. Zhang, C. Hampel and S. Mukerjee, *J. Electrochem. Soc.*, 2005, **152**, A1208.
105 L. Zhang, C. Ma and S. Mukerjee, *J. Electroanal. Chem.*, 2004, **568**, 273.
106 C. Chuy, J. Ding, E. Swanson, S. Holdcroft, J. Horsfall and K. V. Lovell, *J. Electrochem. Soc.*, 2003, **150**, E271.
107 S. Mitsushima, N. Araki, N. Kamiya and K. i. Ota, *J. Electrochem. Soc.*, 2002, **149**, A1370.
108 K. Lee, A. Ishihara, S. Mitsushima, N. Kamiya and K. i. Ota, *J. Electrochem. Soc.*, 2004, **151**, A639.
109 S. Sambandam and V. Ramani, *ECS Trans.*, 2009, **25**, 433.
110 A. Ayad, J. Bouet and J. F. Fauvarque, *J. Power Sources*, 2005, **149**, 66.
111 V. A. Paganin, E. A. Ticianelli and E. R. Gonzalez, *J. Appl. Electrochem.*, 1996, **26**, 297.
112 P. Gode, F. Jaouen, G. Lindbergh, A. Lundblad and G. Sundholm, *Electrochim. Acta*, 2003, **48**, 4175.
113 A. B. Beleke, K. Miyatake, H. Uchida and M. Watanabe, *Electrochim. Acta*, 2007, **53**, 1972.
114 A. Havranek and K. Wippermann, *J. Electroanal. Chem.*, 2004, **567**, 305.
115 M. Eikerling and A. A. Kornyshev, *J. Electroanal. Chem.*, 1999, **475**, 107.
116 H. R. Kunz, V. Mittal, H. Xu, P. Choi and J. Fenton, *Prepr. Symp. - Am. Chem. Soc., Div. Fuel Chem.*, 2007, **52**, 382.
117 N. N. Krishnan, H. J. Kim, J. H. Jang, S. Y. Lee, E. Cho, I. H. Oh, S. A. Hong and T. H. Lim, *J. Appl. Polym. Sci.*, 2009, **113**, 2499.
118 F. Seland, T. Berning, B. Borresen and R. Tunold, *J. Power Sources*, 2006, **160**, 27.
119 R. Fernandez, P. Ferreira-Aparicio and L. Daza, *J. Power Sources*, 2005, **151**, 18.
120 T. H. Yang, Y. G. Yoon, G. G. Park, W. Y. Lee and C. S. Kim, *J. Power Sources*, 2004, **127**, 230.
121 K. Malek, M. Eikerling, Q. Wang, T. Navessin and Z. Liu, *J. Phys. Chem. C*, 2007, **111**, 13627.
122 K. A. Sung, H. Y. Jung, W. K. Kim, K. Y. Cho and J. K. Park, *J. Power Sources*, 2007, **169**, 271.
123 Y. Z. Fu and A. Manthiram, *J. Electrochem. Soc.*, 2007, **154**, B8.
124 R. W. Kopitzke, C. A. Linkous and G. L. Nelson, *Polym. Degrad. Stab.*, 2000, **67**, 335.
125 C. A. Linkous, *Int. J. Hydrogen Energy*, 1993, **18**, 641.
126 A. B. LaConti, M. Hamdan and R. C. McDonald, *Handbook of Fuel Cell Volume 3 Fuel Cell Technology and Applications: Part I*, ed. W. Vielstich, A. Lamm and H. A. Gasteiger, John Wiley & Sons Ltd., England, 2003, ch. 9, p. 547.
127 C. Perrot, G. Meyer, L. Gonon and G. Gebel, *Fuel Cells (Weinheim, Ger.)*, 2006, **6**, 10.
128 C. Perrot, L. Gonon, C. Marestin, A. Morin and G. Gebel, *J. Power Sources*, 2010, **195**, 493.
129 J. Lawrence and T. Yamaguchi, *J. Membr. Sci.*, 2008, **325**, 633.
130 J. Chen, M. Zhai, M. Asano, L. Huang and Y. Maekawa, *J. Mater. Sci.*, 2009, **44**, 3674.
131 V. Sethuraman, J. Weidner, A. Haug and L. Protsailo, *J. Electrochem. Soc.*, 2008, **155**, B119.
132 Z. Chang, H. Pu, D. Wan, L. Liu, J. Yuan and Z. Yang, *Polym. Degrad. Stab.*, 2009, **94**, 1206.
133 J. Lobato, P. Cañizares, M. A. Rodrigo, J. J. Linares and J. A. Aguilar, *J. Membr. Sci.*, 2007, **307**, 47.
134 C. Chen, G. Levitin, D. W. Hess and T. F. Fuller, *J. Power Sources*, 2007, **169**, 288.
135 G. Hubner and E. Roduner, *J. Mater. Chem.*, 1999, **9**, 409.
136 Q. F. Li, H. C. Rudbeck, A. Chromik, J. O. Jensen, C. Pan, T. Steenberg, M. Calverley, N. J. Bjerrum and J. Kerres, *J. Membr. Sci.*, 2010, **347**, 260.
137 B. Vogel, H. Dilger and E. Roduner, *Macromolecules*, 2010, **43**, 4688.
138 C. Genies, R. Mercier, B. Sillion, R. Petiaud, N. Cornet, G. Gebel and M. Pineri, *Polymer*, 2001, **42**, 5097.
139 P. J. Ferreira, G. J. la O, Y. Shao-Horn, D. Morgan, R. Makharia, S. Kocha and H. A. Gasteiger, *J. Electrochem. Soc.*, 2005, **152**, A2256.
140 E. Guilminot, A. Corcella, F. Charlot, F. Maillard and M. Chatenet, *J. Electrochem. Soc.*, 2007, **154**, B96.
141 I. J. Kundler and D. J. Jones, presented in *Carisma Workshop*, Grenoble, France, July 2007.
142 J. Peron, D. J. Jones and J. Roziere, *ECS Trans.*, 2007, **11**, 1313.
143 Y. Yang and S. Holdcroft, *Fuel Cells*, 2005, **5**, 171.
144 M. M. Gross, T. Fuller, S. MacKinnon and C. Gittleman, *Handbook of Fuel Cells Volume 5 and 6 Advances in Electrocatalysis, Materials, Diagnostics and Durability: Part II*, ed. W. Vielstich, H. A. Gasteiger and H. Yokokawa, John Wiley & Sons Ltd., England, 2009, ch. 18, p. 283.
145 E. Antolini, *Appl. Catal., B*, 2009, **88**, 1.